

Quantification of Type VI secretion system activity in macrophages infected with *Burkholderia cenocepacia*

Aubert, D. F., Hu, S., & Valvano, M. A. (2015). Quantification of Type VI secretion system activity in macrophages infected with *Burkholderia cenocepacia*. *Microbiology*, 161(11), 2161-2173. DOI: 10.1099/mic.0.000174

Published in:
Microbiology

Document Version:
Peer reviewed version

Queen's University Belfast - Research Portal:
[Link to publication record in Queen's University Belfast Research Portal](#)

Publisher rights
© 2015 The Authors

General rights
Copyright for the publications made accessible via the Queen's University Belfast Research Portal is retained by the author(s) and / or other copyright owners and it is a condition of accessing these publications that users recognise and abide by the legal requirements associated with these rights.

Take down policy
The Research Portal is Queen's institutional repository that provides access to Queen's research output. Every effort has been made to ensure that content in the Research Portal does not infringe any person's rights, or applicable UK laws. If you discover content in the Research Portal that you believe breaches copyright or violates any law, please contact openaccess@qub.ac.uk.

Microbiology

Quantification of Type VI secretion system activity in macrophages infected with *Burkholderia cenocepacia* --Manuscript Draft--

Manuscript Number:	MIC-D-15-00259R1
Full Title:	Quantification of Type VI secretion system activity in macrophages infected with <i>Burkholderia cenocepacia</i>
Short Title:	Characterization of the <i>B. cenocepacia</i> T6SS
Article Type:	Standard
Section/Category:	Host-microbe interaction
Corresponding Author:	Miguel A Valvano Queen's University Belfast Belfast, UNITED KINGDOM
First Author:	Daniel F. Aubert
Order of Authors:	Daniel F. Aubert Sherry Hu Miguel A Valvano
Abstract:	<p>The Gram-negative bacterial type VI Secretion System (T6SS) delivers toxins to kill or inhibit the growth of susceptible bacteria, while others target eukaryotic cells. Deletion of <i>atsR</i>, a negative regulator of virulence factors in <i>B. cenocepacia</i> K56-2, increases T6SS activity. Macrophages infected with a K56-2 Δ<i>atsR</i> mutant display dramatic alterations in their actin cytoskeleton architecture that rely on the T6SS, which is responsible for the inactivation of multiple Rho-family GTPases by an unknown mechanism. We employed a strategy to standardize the bacterial infection of macrophages and densitometrically quantify the T6SS-associated cellular phenotype, which allowed us to characterize the phenotype of systematic deletions of each gene within the T6SS cluster and ten <i>vgrG</i> encoding genes in K56-2 Δ<i>atsR</i>. None of the genes from the T6SS core cluster and the individual <i>vgrG</i>s were directly responsible for the cytoskeletal changes in infected cells. However, a mutant strain with all <i>vgrG</i> genes deleted was unable to cause macrophage alterations. Despite not being able to identify a specific effector protein responsible for the cytoskeletal defects in macrophages, our strategy resulted in the identification of the critical core components and accessory proteins of the T6SS assembly machinery and provides a screening method to detect T6SS effectors targeting the actin cytoskeleton in macrophages by random mutagenesis.</p>

1

2

3

4 **Quantification of Type VI secretion system activity in macrophages infected with**

5 *Burkholderia cenocepacia*

6

7 **Daniel F. Aubert¹, Sherry Hu¹ and Miguel A. Valvano^{1,2}**

8

9 ¹ Department of Microbiology and Immunology, University of Western Ontario, London,

10 Ontario N6A 5C1, Canada;

11 ² Centre for Infection and Immunity, Queen's University Belfast, BT9 5GZ, Belfast,

12 United Kingdom

13

14 Running title: Characterization of the *B. cenocepacia* T6SS

15

16 Key words: T6SS, core component, VgrG, effector protein, *Burkholderia cenocepacia*

17

18

19 Correspondence: Miguel A. Valvano, m.valvano@qub.ac.uk

20

21 **ABSTRACT**

22 The Gram-negative bacterial type VI Secretion System (T6SS) delivers toxins to kill or
23 inhibit the growth of susceptible bacteria, while others target eukaryotic cells. Deletion of
24 *atsR*, a negative regulator of virulence factors in *B. cenocepacia* K56-2, increases T6SS
25 activity. Macrophages infected with a K56-2 Δ *atsR* mutant display dramatic alterations in
26 their actin cytoskeleton architecture that rely on the T6SS, which is responsible for the
27 inactivation of multiple Rho-family GTPases by an unknown mechanism. We employed
28 a strategy to standardize the bacterial infection of macrophages and densitometrically
29 quantify the T6SS-associated cellular phenotype, which allowed us to characterize the
30 phenotype of systematic deletions of each gene within the T6SS cluster and ten *vgrG*
31 encoding genes in K56-2 Δ *atsR*. None of the genes from the T6SS core cluster and the
32 individual *vgrGs* were directly responsible for the cytoskeletal changes in infected cells.
33 However, a mutant strain with all *vgrG* genes deleted was unable to cause macrophage
34 alterations. Despite not being able to identify a specific effector protein responsible for
35 the cytoskeletal defects in macrophages, our strategy resulted in the identification of the
36 critical core components and accessory proteins of the T6SS assembly machinery and
37 provides a screening method to detect T6SS effectors targeting the actin cytoskeleton in
38 macrophages by random mutagenesis.
39

40 INTRODUCTION

41 *Burkholderia cenocepacia* is an environmental Gram-negative opportunistic pathogen
42 that causes persistent, often severe, lung infections in individuals with cystic fibrosis (CF)
43 and other underlying diseases (Drevinek & Mahenthiralingam, 2010; Isles *et al.*, 1984;
44 Mahenthiralingam *et al.*, 2008). Infections by this bacterium are difficult to treat due to
45 the intrinsic and high-level multidrug resistance of *B. cenocepacia* to most clinically
46 relevant antibiotics (Waters, 2012). Also, *B. cenocepacia* can be transmitted from patient
47 to patient (Drevinek & Mahenthiralingam, 2010). *B. cenocepacia* is pathogenic in several
48 plant and non-mammalian animal infection models (Khodai-Kalaki *et al.*, 2015; Thomson
49 & Dennis, 2013; Uehlinger *et al.*, 2009; Vergunst *et al.*, 2010) and can survive
50 intracellularly within epithelial cells (Burns *et al.*, 1996; Sajjan *et al.*, 2006),
51 macrophages (Lamothe *et al.*, 2007; Martin & Mohr, 2000; Saini *et al.*, 1999) and
52 amoebae (Lamothe *et al.*, 2004; Marolda *et al.*, 1999).

53

54 The Type VI secretion system (T6SS) is widely distributed among Gram-negative
55 bacteria (Costa *et al.*, 2015; Zoued *et al.*, 2014). It forms an elongated protein complex,
56 which is structurally related to the tail-tube and puncturing device of bacteriophages
57 (Shneider *et al.*, 2013; Zoued *et al.*, 2014). The T6SS is an extremely dynamic contractile
58 nanomachine (Basler *et al.*, 2012; Bonemann *et al.*, 2010; Clemens *et al.*, 2015;
59 Kudryashev *et al.*, 2015) that attacks cells by initially penetrating them with a trimeric
60 protein complex called the VgrG spike. The spike first assembles into a membrane-
61 anchored complex formed of an inner tail tube made of Hcp proteins surrounded by an
62 outer sheath VipA- and VipB-like proteins (Bonemann *et al.*, 2009). In turn, proteins

63 from the PAAR (proline-alanine-alanine-arginine) repeat superfamily bind to the VgrGs
64 and are essential for T6SS-mediated secretion into other bacterial cells, forming a spike
65 complex decorated with multiple effectors that are delivered simultaneously into target
66 cells through a contraction-driven translocation event (Shneider *et al.*, 2013). The AAA+
67 ATPase ClpV disassembles the outer sheath complex, a process that requires ATP
68 hydrolysis, and then the inner Hcp tube is detached and released into the medium
69 (Bonemann *et al.*, 2009). The T6SS, now referred to as a bacterial poison dagger, is a
70 versatile weapon, which requires intimate cell contact to deliver a wide range of toxins
71 into bacterial competitors or eukaryotic cells. Most identified T6SS effector proteins act
72 on bacterial cells and include peptidoglycan-degrading enzymes, membrane-degrading
73 lipases, and nucleic acid targeting enzymes (Durand *et al.*, 2014; Russell *et al.*, 2014). In
74 some cases, the same effector can function in bacterial antagonism and also alters cell-
75 signaling pathways in eukaryotic cells (Jiang *et al.*, 2014). Also, “evolved” VgrGs have
76 been described that contain various C-terminal extensions leading for instance to actin-
77 crosslinking or actin-ADP-ribosylation in eukaryotic cells (Brooks *et al.*, 2013; Pukatzki
78 *et al.*, 2007; Suarez *et al.*, 2010), and host cell fusion presumably to facilitate intercellular
79 bacterial spreading (Schwarz *et al.*, 2014; Toesca *et al.*, 2014).

80

81 The T6SS of *B. cenocepacia* K56-2 was first identified in a signature-tagged mutagenesis
82 study pointing out the importance of this secretion system for *B. cenocepacia* survival in
83 a rat model of chronic respiratory infection (Aubert *et al.*, 2008; Hunt *et al.*, 2004). Study
84 of *B. cenocepacia* T6SS *in vitro* was rendered possible by the discovery of AtsR
85 (Adhesion and Type Six secretion system Regulator), a hybrid sensor kinase that

86 negatively regulates the expression of *B. cenocepacia* virulence factors including the
87 T6SS (Aubert *et al.*, 2010; Aubert *et al.*, 2008; Aubert *et al.*, 2013; Khodai-Kalaki *et al.*,
88 2013). Deletion of *atsR* causes a significant increase in T6SS activity, as denoted by
89 increased amounts of Hcp released into bacterial culture supernatant (Aubert *et al.*,
90 2008), induction of actin cytoskeletal rearrangements in infected macrophages (Aubert *et*
91 *al.*, 2008; Flannagan *et al.*, 2012; Rosales-Reyes *et al.*, 2012), and delayed assembly of
92 the NADPH oxidase complex at the membrane of the *B. cenocepacia*-containing vacuole
93 (Keith *et al.*, 2009; Rosales-Reyes *et al.*, 2012). These cellular defects in infected
94 macrophages are characteristic for *B. cenocepacia* and depend on T6SS-mediated defects
95 in the activation of multiple Rho family GTPases by an unknown mechanism presumably
96 via unknown T6SS effector molecules (Flannagan *et al.*, 2012; Rosales-Reyes *et al.*,
97 2012). Here we show that Hcp detection in bacterial culture supernatants and
98 quantification of the morphological phenotype in infected macrophages allowed us to
99 characterize the components of the T6S apparatus in *B. cenocepacia* required for T6SS
100 function and to refine the boundaries of the T6SS cluster. The relevance of *B.*
101 *cenocepacia* VgrG proteins for T6SS function and T6SS-related phenotype was also
102 investigated. From our results, we propose that quantification of the morphological
103 phenotype in macrophages is a sensitive and reproducible test that can serve as a
104 screening tool to identify mutations denoting *B. cenocepacia* genes that are responsible
105 for disturbing the actin cytoskeleton in infected macrophages.

106

107

108 **METHODS**

109 **Bacterial strains, plasmids, and culture media.** Bacterial strains and plasmids used in
110 this study are listed in Table 1. Bacteria were grown in Luria Broth (LB) (Difco) at 37°C.
111 *Escherichia coli* cultures were supplemented, as required, with the following antibiotics
112 (final concentrations): 30 µg tetracycline ml⁻¹, 30 µg kanamycin ml⁻¹, and 50 µg
113 trimethoprim ml⁻¹. *B. cenocepacia* cultures were supplemented, as required, with 100 µg
114 trimethoprim ml⁻¹ and 100 µg tetracycline ml⁻¹.

115

116 **General molecular techniques.** DNA manipulations were performed as described
117 previously (Sambrook *et al.*, 1990). T4 DNA ligase (Roche Diagnostics, Laval, Quebec,
118 Canada) and Antarctic phosphatase (New England Biolabs, Pickering, Ontario, Canada)
119 were used as recommended by the manufacturers. Transformation of *E. coli* DH5α and *E.*
120 *coli* GT115 was done using the calcium chloride method (Cohen *et al.*, 1972).
121 Mobilization of complementing plasmids and mutagenesis plasmids into *B. cenocepacia*
122 was performed by triparental mating using *E. coli* DH5α carrying the helper plasmid
123 pRK2013 (Craig *et al.*, 1989; Figurski & Helinski, 1979). DNA amplification by
124 polymerase chain reaction (PCR) was performed using a PTC-221 DNA engine (MJ
125 Research, Incline Village, Nevada) with Taq or HotStar HiFidelity DNA polymerases
126 (Qiagen Inc., Mississauga, Ontario, Canada). DNA sequences of all primers used in this
127 study are described in the Supplemental Table S2. DNA sequencing was performed at the
128 DNA sequencing Facility of York University, Toronto, Canada. The KEGG database
129 (Kanehisa & Goto, 2000) and the computer program BLAST (Altschul *et al.*, 1990) were
130 used to analyze the sequenced genome of *B. cenocepacia* strains K56-2 and J2315.

131

132 **Deletion mutagenesis of *B. cenocepacia* K56-2 and complementing plasmids.**

133 Oligonucleotide primers used for the construction of mutagenic and complementing
134 plasmids are listed in Table S1, and the plasmids construction details are provided in
135 Supplementary data. Unmarked and non-polar deletions were performed as described
136 previously (Flannagan *et al.*, 2008; Hamad *et al.*, 2010). All deletion plasmids were
137 introduced into *E. coli* GT115 by transformation and mobilized into *B. cenocepacia* by
138 triparental mating. When gentamicin-sensitive strains were used, *E. coli* counter-selection
139 was performed with 200 µg carbenicillin ml⁻¹ and 10 µg polymyxin B ml⁻¹ instead of 50
140 µg gentamicin ml⁻¹. Gene deletions were confirmed by PCR. Mutants were tested in a
141 Bioscreen C automated microbiology growth curve analysis system at 37°C, with
142 continuous shaking and OD₆₀₀ measurements taken every hour as described previously
143 (Aubert *et al.*, 2008).

144

145 **Expression and purification of His-tagged Hcp and polyclonal antibody**

146 **preparations.** *hcp* was PCR amplified with primers 2143 and 2748 and cloned into
147 plasmid pET30a using *NdeI* and *HindIII* restriction sites. This generated plasmid pDA44
148 encoding Hcp_{6xHis}, which was introduced into *E. coli* strain BL21 (DE3) by
149 transformation. Overexpression of Hcp_{6xHis} was performed as follows. *E. coli* cells were
150 grown to an OD₆₀₀ of 0.6, induced with 0.05 mM isopropyl-β-d-1-thiogalactopyranoside
151 (IPTG), and grown for another 2 h at 30°C. Cells were collected by centrifugation and
152 resuspended in 50 mM sodium phosphate pH 7.4, 300 mM NaCl, and lysed using a
153 French press. Debris were removed following centrifugation at 20 000 ×g for 20 min.

154 Hcp_{6xHis} was purified from filtered supernatant by FPLC (ÄKTA Basic instrument) using
155 a 5 ml HisTrap column (GE Healthcare). Elution was performed using a linear gradient
156 concentration of imidazole (10-400 mM). Fractions containing purified Hcp_{6xHis} were
157 pooled and dialyzed against 50 mM sodium phosphate, pH 7.4, 300 mM NaCl, and stored
158 at 4°C. The eluted Hcp_{6xHis} was judged >90% pure after this step. Polyclonal antibodies
159 recognizing Hcp were generated in New Zealand White rabbits by ProSci Inc. (Poway,
160 CA).

161

162 **Precipitation of culture supernatant proteins and immunoblot analysis.** Culture
163 supernatant proteins were precipitated as described previously (Aubert *et al.*, 2008) with
164 some modifications. Briefly, overnight cultures were diluted to an OD₆₀₀ of 0.03 in pre-
165 warmed LB and grown until early exponential phase, at which time OD₆₀₀ was also
166 recorded. Proteins from filter-sterilized culture supernatants were precipitated overnight
167 at 4 °C using 20% trichloroacetic acid (final concentration). Five µg of secreted proteins
168 were loaded on an 18% SDS-PAGE. The crude lysate sample (pellet fraction) was
169 prepared as follows: bacteria from 1 ml of exponential phase culture adjusted at an OD₆₀₀
170 of 0.5 were pelleted by centrifugation, resuspended into 30 µl of 1x protein loading dye
171 and boiled for 10 min. Samples were centrifuged for 3 min at 5 900 ×g and 3 µl of total
172 cell lysate were loaded on a 18% SDS-PAGE. After electrophoresis, gels were transferred
173 to nitrocellulose membranes for immunoblot analysis. After blocking (Roche), the
174 membranes were incubated with the following primary antibodies as required. 4RA2
175 monoclonal antibody (Neoclone), which cross-reacts with the *B. cenocepacia* and *B.*
176 *multivorans* RNA polymerase subunit alpha (cytosolic / cell lysis control) (dilution of

177 1:25 000), anti-Hcp polyclonal antiserum (ProSci-inc) (dilution of 1:1 000) and FLAG
178 M2 monoclonal antibody (Sigma) (dilution of 1:50 000). Secondary antibodies Alexa
179 Fluor 680 conjugated goat anti-mouse IgG (Molecular Probes) and IRDye800 conjugated
180 goat anti-rabbit IgG (Rockland) were used at a dilution of 1:50 000. Detection was
181 performed using the Odyssey Infrared Imager (LI-COR Biosciences).

182

183 **Macrophage infections and quantification of the T6SS activity.** Infections were
184 performed as previously described (Aubert *et al.*, 2008) using the C57BL/6 murine bone
185 marrow-derived macrophage cell line ANA-1 (Cox *et al.*, 1989). Bacteria were washed
186 three times with DMEM 10% FBS and added to ANA-1 cells grown on glass coverslips
187 at a MOI of 50:1. Plates were centrifuged for 2 min at 300 ×g to synchronize the infection
188 and incubated at 37°C under 5% CO₂. Coverslips were analyzed by phase contrast
189 microscopy at 4 h post-infection. T6SS activity was recorded as the ability of the bacteria
190 to induce the formation of characteristic ectopic structures around the macrophages
191 (Aubert *et al.*, 2008). An assay was developed to measure the extent of the formation of
192 these structures around the macrophages. As “beads on a string-like” structures appear as
193 dark objects on a clear background around macrophages in phase contrast microscopy the
194 percentage of the area occupied by dark objects can be measured upon picture analysis
195 using the Northern Eclipse software. For each infection, pictures with a 100x
196 magnification were taken under the same conditions of light, gain and exposure. A
197 threshold was applied to highlight the dark pixels on the images and the number of
198 macrophages and Percent of object Area values for each image was recorded. The
199 intensity of T6SS activity was calculated for each mutant by dividing the sum of the

200 Percent Area values measured over at least 21 fields of view by the total number of
201 macrophages (over 300 macrophages). The ability to induce the formation of “beads on a
202 string-like” structures around macrophages, which is representative of the T6SS activity
203 in each mutant, was expressed in arbitrary units relative to $\Delta atsR$ set as 1. Experiments
204 were repeated independently three times. Uninfected ANA-1 cells were used as a
205 negative control to determine background levels. The negative control had 0.1 ± 0.02
206 relative units. Therefore, experimental samples giving relative units equal or lower than
207 0.2 (corresponding to 5 standard deviation units from the mean of the negative control)
208 were considered as indicative of cells lacking ectopic structures. One-way Anova (Prism
209 5.0a, GraphPad Software Inc.) was utilized to analyze the data from the quantification
210 experiments. The Bonferroni Multiple Comparison test using a significance level of 0.01
211 was used to compare the relative units obtained from experimental samples and
212 uninfected controls.

213

214 **Gentamicin protection assay.** Bacterial infection and bacterial intracellular survival
215 were assayed as described previously (Schmerk & Valvano, 2013) with slight
216 modifications. ANA-1 macrophages were seeded in 12-well plates at a density of 3×10^5
217 cells per well and incubated overnight. Gentamicin sensitive strains were grown
218 overnight in LB broth at 37°C with shaking. Bacteria were used to infect ANA-1
219 macrophages at a MOI of 50:1 as described above. One hour post-infection, macrophages
220 were washed with PBS three times to remove extracellular bacteria. DMEM 10% FBS
221 containing $100 \mu\text{g gentamicin ml}^{-1}$ was added to kill remaining extracellular bacteria.
222 One hour later, macrophages were washed twice in PBS, and fresh medium containing 10

223 μg gentamicin ml^{-1} was added for the remainder of the experiment. To enumerate
224 intracellular bacteria, infected macrophages were lysed with 0.1% sodium deoxycholate
225 (w/v) at 4 h post-infection. Lysates were serially diluted in PBS and plated on LB agar.

226

227 **RESULTS**

228

229 **Functional characterization of the T6SS components of *B. cenocepacia* K56-2**

230 The genome of *B. cenocepacia* K56-2 contains only one T6SS locus on chromosome 1
231 (spanning 23.7 kilobase pairs) (Fig. 1a). The boundaries of the T6SS locus in *B.*
232 *cenocepacia* K56-2 were initially set from BCAL0352 up to BCAL0333 because of its
233 immediate location upstream of a tRNA sequence (as observed in pathogenicity islands)
234 and based on the identification of three putative transcriptional units containing
235 conserved T6SS components (Aubert *et al.*, 2010; Boyer *et al.*, 2009). Unlike many other
236 bacteria (Boyer *et al.*, 2009), the putative T6SS cluster of *B. cenocepacia* K56-2 does not
237 contain any *vgrG* (Fig. 1a). The predicted functions of the T6SS genes are listed in the
238 Supplemental Table S2, and whenever possible the genes were named according to the
239 proposed standard nomenclature for T6SS core components, *tss* (for T6SS gene) or *tag*
240 (T6SS-associated gene) (Shalom *et al.*, 2007). Each of the genes in the T6SS cluster was
241 systematically deleted in *B. cenocepacia* Δ *atsR* and the mutants investigated for T6SS
242 related phenotypes. All mutants had similar growth rates compared to the wild type strain
243 (data not shown). As previously demonstrated (Aubert *et al.*, 2008), infection of ANA-1
244 macrophages with Δ *atsR* induces the formation of “beads on a string-like” structures due
245 to lamellipodia collapse and impairment of actin-tail retraction during macrophage
246 migration (Flannagan *et al.*, 2012; Rosales-Reyes *et al.*, 2012) (Fig. 1b). This phenotype
247 depends on a functional T6SS, as Δ *atsR* Δ *hcp* cannot disturb the cytoskeleton
248 organization (Aubert *et al.*, 2008; Rosales-Reyes *et al.*, 2012). The nature of the secreted

249 effector eliciting changes in actin architecture is still unknown. In an attempt to determine
250 whether a gene encoding an effector lied within the T6SS cluster, mutants were first
251 evaluated for their ability to induce cytoskeletal rearrangements in infected macrophages
252 and then for their ability to release Hcp into culture supernatants (denoting a functional
253 T6SS). An assay was developed to quantify the T6SS activity by measuring the extent of
254 the formation of “beads on a string-like” structures. Since these structures appear around
255 macrophages as dark objects on a clear background in phase contrast microscopy (Fig.
256 1b) it is possible to measure the area they occupy per field of view using image analysis
257 software. The “amount” of dark objects, which is representative of the intensity of T6SS
258 activity, was calculated (see Methods) for each mutant tested and expressed relative to
259 Δ *atsR* (Fig. 1c). Uninfected cells were used as negative control to determine the
260 background level. Relative units below 0.2 (corresponding to 5 standard deviation units
261 from the mean) were considered as indicative of cells lacking ectopic structures and
262 consequently infected with T6SS-defective strains.

263

264 Deletion mutants lacking *tssM* (BCAL0351; *icmF*-like), *tssA* (BCAL0348), *tssH*
265 (BCAL0347; *clpV*-like), *tssG* (BCAL0346), *tssF* (BCAL0345), *tssE* (BCAL0344), *tssD*
266 (BCAL0343; *hcp*-like), *tssC* (BCAL0342; *bcsK_C*), *tssB* (BCAL0341; *bcsL_B*), *tssK*
267 (BCAL0338) or *tssL* (BCAL0337) did not produce visible ectopic structures around
268 macrophages. Therefore, the calculated relative units were not significantly different than
269 those of uninfected cells, indicating that the deleted genes encode critical components for
270 the T6SS activity (Fig. 1c). The mutant with a deletion of BCAL0340 was able to induce
271 the formation of ectopic structures around macrophages at very low levels (0.27 ± 0.02

272 relative units), but the results did not show a significant difference compared to
273 uninfected cells. In contrast, mutants carrying a deletion in BCAL0352, *tagF*
274 (BCAL0350), *tagL* (BCAL0349), *tssJ* (BCAL0339), and BCAL0336-33 were able to
275 induce the formation of ectopic structures around macrophages, resulting in significantly
276 different relative units compared to the uninfected control ($p < 0.001$), suggesting that
277 these genes encode proteins dispensable for T6SS activity under the conditions assayed
278 here.

279

280 Mutants were also evaluated for their ability to export and release Hcp into culture
281 supernatants. As previously demonstrated (Aubert *et al.*, 2010; Aubert *et al.*, 2008), Hcp
282 is clearly detected in culture supernatants from $\Delta atsR$ denoting a functional T6S
283 machinery (Fig. 1d). Most of the genes located within the T6SS cluster were required for
284 Hcp export. Mutants carrying a deletion in *tssM*, *tssA*, *tssH*, *tssG*, *tssF*, *tssE*, *tssC*, *tssB*,
285 BCAL0340, *tssK* or *tssL* were unable to export Hcp, while mutants with a deletion in
286 BCAL0352, *tagL* or *tssJ* had reduced levels of Hcp exported into the culture supernatants
287 as compared to $\Delta atsR$. These results also agree with the observation that these three
288 mutants reproducibly induced lower levels of ectopic structures in macrophages in
289 comparison with $\Delta atsR$ (0.71, 0.72, and 0.55 relative units; Fig. 1c), suggesting that the
290 encoded proteins probably have an effect on the overall efficiency of the T6SS. In
291 contrast, similar levels of Hcp were detected in $\Delta atsR\Delta BCAL0336-33$ and $\Delta atsR$ culture
292 supernatants. Besides $\Delta atsR\Delta hcp$, the intracellular levels of Hcp were similar for all
293 mutants tested except for $\Delta atsR\Delta tagF$, which repeatedly displayed lower levels of
294 cytosolic Hcp but higher levels of exported Hcp compared to $\Delta atsR$ (Fig. 1d).

295

296 These results show that there is in most cases, a good correlation between Hcp export
297 levels and T6SS activity as measured by the extent of the formation of “beads on a string-
298 like” structures. Together, these assays identified *tssM*, *tssA*, *tssH*, *tssG*, *tssF*, *tssE*,
299 *tssD(hcp)*, *tssC*, *tssB*, BCAL0340, *tssK* and *tssL* as core components of the T6S
300 machinery, which are critical for assembly and function, and BCAL0352, *tagL* and *tssJ*
301 as accessory proteins likely involved in the stability of the T6SS complex or required for
302 its proper functioning. None of the mutants tested were unable to elicit changes in
303 macrophages morphology while retaining the ability to export Hcp, suggesting that the
304 gene encoding the effector molecule responsible for cytoskeletal rearrangements is not
305 located within the T6SS cluster.

306

307 **Characterization of BCAL0345 paralogs**

308 We investigated the presence of paralogs of the T6SS genes using the KEGG database for
309 the *B. cenocepacia* strain J2315 ([http://www.genome.jp/kegg-](http://www.genome.jp/kegg-bin/show_organism?org=bcj)
310 [bin/show_organism?org=bcj](http://www.genome.jp/kegg-bin/show_organism?org=bcj)), which is a clonal isolate with K56-2 (Mahenthiralingam *et*
311 *al.*, 2000). For each gene of the T6SS, paralogs were investigated according to the
312 threshold values given for the Smith-Waterman algorithm (Smith & Waterman, 1981), as
313 automatically provided by the KEGG database. We found that the genes located in the
314 T6SS locus were unique within *B. cenocepacia* except for *tssF* and *tssH*. Each of them
315 has two paralogs BCAL1293/BCAS0668 (in chromosome 3) and
316 BCAL1919/BCAL2730, respectively. BCAL1919 and BCAL2730 were not further
317 investigated as they encode the well-characterized ClpB heat-shock protein and ATP-

318 binding subunit ClpA from the ATP-dependent Clp protease, respectively. Interestingly,
319 BCAL1293 and BCAS0668 were located immediately next to a VgrG encoding gene
320 (BCAL1294 and BCAS0667). The amino acid sequences of BCAL1293 and BCAS0668
321 are 42% and 40% identical (58% and 54% similar) to TssF, respectively (Fig. S1).
322 BCAL1293 and BCAS0668 were individually deleted in $\Delta atsR$ and mutants were tested
323 for T6SS activity in our macrophage infection model. In contrast to $\Delta atsR\Delta tssF$,
324 $\Delta atsR\Delta BCAL1293$ and $\Delta atsR\Delta BCAS0668$ could elicit morphological changes in
325 macrophages at similar levels to $\Delta atsR$ (Fig. 2). Introduction of plasmid pL0345
326 (encoding TssF) into $\Delta atsR\Delta BCAL0345$ restored T6SS activity, however introduction of
327 plasmids pL1293 or pS0668 (expressing BCAL1293 or BCAS0668, respectively) did not
328 (Fig. 2). These results suggest that although BCAL1293 or BCAS0668 are paralogs of
329 the critical core component TssF, they are not required for T6SS activity under the
330 conditions assayed here, as they cannot functionally replace TssF.

331

332 **Identification and characterization of the VgrGs of *B. cenocepacia* K56-2**

333 The N-terminus of a VgrG element contains two conserved domains, Phage_GPD and
334 Phage_base_V (former DUF586), which are related to the bacteriophage T4 tail spike
335 protein gp27 (Pukatzki *et al.*, 2007). Computer-assisted analysis using the sequence of
336 the Phage_base_V motif from VgrG2 (VCA0018 from *V. cholerae*) as query identified
337 ten VgrGs (BCAL1165, BCAL1294, BCAL1355, BCAL1359, BCAL1362, BCAL2279,
338 BCAM0043, BCAM0148, BCAM2254, and BCAS0667) in the sequenced genome of *B.*
339 *cenocepacia* K56-2 (Varga *et al.*, 2013)(GenBank accession number
340 NZ_ALJA00000000.2) (Fig. 3). The *vgrGs* were scattered over the three chromosomes

341 and none of them was localized in or at the vicinity of the T6SS cluster. BCAM2279 has
342 an insertion sequence (IS) inserted at the very end of the gene; however, the encoded
343 VgrG might still be functional since only the last 17 amino acids are missing and
344 replaced by 22 amino acids provided by the IS, which are followed by a stop codon. Psi-
345 BLAST and PFAM analysis revealed that these VgrGs also contains the Phage_GPD
346 domain and other motifs classically found in VgrG proteins such as T6SS_Vgr, Gp5_C
347 repeats and DUF2345 (Fig. 3). None of them displayed C-terminal extensions with
348 homologies to domains found in previously characterized “evolved” VgrGs (e.g. actin-
349 crosslinking domain, ADP-ribosylation domain, peptidoglycan-binding domain). Instead,
350 conserved domain predictions identified a C-terminal extension in the two largest VgrGs,
351 BCAL1359 (1233 aa) and BCAS0667 (999 aa), which carry a M6 family metalloprotease
352 domain with a characteristic HExxH motif (E-value: 7.18e-03) and a putative lipase_3
353 domain (GxSxG motif, E-value: 2.8e-02) found in triglyceride lipase, respectively.

354

355 Each *vgrG* gene was individually deleted in *B. cenocepacia* Δ *atsR* and growth curves
356 analyses indicated that all mutants had similar growth rates (data not shown). Mutants
357 were then tested for their ability to induce cytoskeleton rearrangements in infected
358 macrophages and to export Hcp into culture supernatants (Fig. 4a-b). Single *vgrG*
359 deletions did not affect either Hcp export or morphological changes in macrophages
360 denoting T6SS activity, suggesting that none of the individual VgrGs are critical for
361 T6SS function. Although we cannot rule out that the evolved VgrGs BCAL1359 and
362 BCAS0667 are T6SS effectors, they can be excluded from an involvement in actin
363 cytoskeleton alterations. A VgrG-less strain was created in *B. cenocepacia* Δ *atsR*.

364 Deletion of the 10 *vgrG* genes resulted in a non-functional T6SS unable to cause the actin
365 cytoskeleton phenotype in infected macrophages or export Hcp (Fig. 4c), indicating that
366 multiple VgrGs are nevertheless required for the changes in macrophage morphology that
367 are characteristics of *B. cenocepacia* T6SS function.

368

369 **DISCUSSION**

370 This study aimed to characterize the *B. cenocepacia* T6SS using two assays indicative of
371 T6SS function: Hcp secretion and quantification of the morphological defects in infected
372 macrophages. Deletion of most genes in the *B. cenocepacia* T6SS cluster resulted in
373 strains unable to export Hcp. These results were not surprising since with the exception
374 of BCAL0340, orthologs of all the genes annotated as critical components in our study
375 were also identified as genes encoding conserved core subunits essential for the T6
376 secretory functions in other bacteria (Durand *et al.*, 2012; English *et al.*, 2014; Zheng &
377 Leung, 2007; Zheng *et al.*, 2011; Zoued *et al.*, 2013). However, one major difference
378 concerned the *tssJ*-like BCAL0339. In enteroaggregative *E. coli*, *V. cholerae* and
379 *Edwardsiella tarda*, *tssJ* encodes an outer membrane lipoprotein that interacts with TssM
380 and is critical for Hcp export (Aschtgen *et al.*, 2008; Felisberto-Rodrigues *et al.*, 2011;
381 Zheng & Leung, 2007; Zheng *et al.*, 2011). In *B. cenocepacia*, TssJ_{Bc} is not essential,
382 although it is required for optimum Hcp export and T6SS activity. While this remains to
383 be tested, it is possible that an additional component encoded within the *B. cenocepacia*
384 T6SS cluster exerts a function similar to that of TssJ_{Bc}. BCAL0340 (NOG73587) could
385 be such a candidate. Like TssJ_{Bc}, BCAL0340 is predicted to be a lipoprotein, and
386 contains tetratricopeptide repeats indicating that it is likely involved in protein-protein
387 interaction. BCAL0340 is highly conserved among the T6SS clusters in *Burkholderia*
388 species but infrequently found in T6SS clusters from other bacteria (Boyer *et al.*, 2009).
389 It is also absent from the T6SS clusters from enteroaggregative *E. coli*, *V. cholerae* and
390 *Edwardsiella tarda*. In contrast to TssJ_{Bc}, our results demonstrate that BCAL0340 is a
391 critical component of the *B. cenocepacia* T6SS, since deletion of BCAL0340 abolished

392 Hcp export and also prevented the "beads on a string" phenotype in infected
393 macrophages.

394

395 Like BCAL0340, BCAL0352 is another gene not frequently found within T6SS clusters
396 (Boyer *et al.*, 2009), and it is also highly conserved among the T6SS clusters of
397 *Burkholderia* species. BCAL0352 (NOG43466) encodes a putative membrane anchored
398 M15C metallopeptidase possibly with L-alanyl-D-glutamate endopeptidase activity,
399 which suggests an involvement in peptidoglycan degradation that is reminiscent of the
400 Tse toxins involved in bacterial competition (Russell *et al.*, 2011). However, the effect of
401 BCAL0352 deletion on Hcp export, the presence of a N-terminal signal peptide and one
402 transmembrane domain in the encoded protein argue against a putative effector role.
403 Although previous data in our laboratory indicated that BCAL0352 and BCAL0351 are
404 co-transcribed (Aubert & Valvano, unpublished), it is also possible that deletion of
405 BCAL0352 affects additional promoter sequences required for optimum T6SS
406 expression.

407

408 TagF (BCAL0350) is conserved in 30% of the identified T6SS clusters (Boyer *et al.*,
409 2009), but it was dispensable for T6SS activity in *B. cenocepacia*. Interestingly, deletion
410 of *tagF* led to decreased endogenous Hcp pool and a corresponding increase in Hcp
411 release into culture supernatants. These observations suggest that TagF might have a role
412 in the turnover of the Hcp channel. TagL (BCAL0349) is conserved in 25% of the T6SS
413 clusters (Boyer *et al.*, 2009) and encodes a putative outer membrane protein with an
414 OmpA motif (E value 4.4e-25) and the PF0691 motif, which is characteristic of cell wall

415 binding protein components of T6SSs (Aschtgen *et al.*, 2010). TagL may have an
416 accessory function, which can be important for the proper production, assembly, or
417 activity of the T6S apparatus. Further, our results ruled out the small ORFs (BCAL0333-
418 BCAL0336) as genes encoding either potential T6SS effectors involved in the eukaryotic
419 phenotype or components influencing T6SS functioning. Therefore, we have reassigned
420 the boundaries of the *B. cenocepacia* T6SS cluster to only include 16 genes (BCAL0352-
421 *tssL*)(Fig. 1a).

422

423 Individual deletion of any of the 10 VgrGs identified in *B. cenocepacia* K56-2 did not
424 alter Hcp export or the ability of the mutant strain to produce morphological changes in
425 macrophages, suggesting these proteins have redundant function. Whether the two VgrGs
426 with a C-terminal extension (BCAL1359 and BCAS0667) are effectors involved in other
427 T6SS functions such as bacterial competition will require additional experimentation.
428 VgrGs are also structural components of the T6S machinery and as part of the base-plate
429 complex they are required for the initiation of the Hcp tube polymerization (Basler *et al.*,
430 2012). As expected, deletion of the 10 *vgrGs* in Δ *atsR* abolished Hcp export and T6SS
431 activity. Although the effect of successive *vgrG* deletions was not investigated, these
432 results confirm that at least several of the *B. cenocepacia* VgrGs are critical for the T6SS
433 function. Most of the 10 VgrGs likely have redundant functions, suggesting their
434 relevance in T6SS assembly presumably depends on their nature and relative expression
435 levels. In summary, we have characterized core components of the *B. cenocepacia* T6SS.
436 Our results indicate that none of these components are directly responsible for inducing
437 actin cytoskeletal changes in macrophages. However, the quantitative approach we have

438 developed to investigate macrophage cell morphology can be adapted for screening
439 random mutants in the search for one or more T6SS effector proteins acting on Rho-type
440 GTPases, which is currently underway in our laboratory.

441

442 **ACKNOWLEDGEMENTS**

443 The authors thank W. Cladman for purification of the Hcp protein used for immunization
444 and M.S. Saldías and C. Schmerk for critical review of the manuscript. This work was
445 supported by grants from Cystic Fibrosis Canada and the U.K. Cystic Fibrosis Trust (to
446 M.A.V).

447

448

449 REFERENCES

450 Altschul, S. F., Gish, W., Miller, W., Myers, E. W. & Lipman, D. J. (1990). Basic
451 local alignment search tool. *J Mol Biol* **215**, 403-410.

452

453 Aschtgen, M. S., Bernard, C. S., De Bentzmann, S., Lloubes, R. & Cascales, E.
454 (2008). SciN is an outer membrane lipoprotein required for type VI secretion in
455 enteroaggregative *Escherichia coli*. *J Bacteriol* **190**, 7523-7531.

456

457 Aschtgen, M. S., Thomas, M. S. & Cascales, E. (2010). Anchoring the type VI
458 secretion system to the peptidoglycan: TssL, TagL, TagP... what else? *Virulence* **1**, 535-
459 540.

460

461 Aubert, D., MacDonald, D. K. & Valvano, M. A. (2010). BcsK_C is an essential protein
462 for the type VI secretion system activity in *Burkholderia cenocepacia* that forms an outer
463 membrane complex with BcsL_B. *J Biol Chem* **285**, 35988-35998.

464

465 Aubert, D. F., Flannagan, R. S. & Valvano, M. A. (2008). A novel sensor kinase-
466 response regulator hybrid controls biofilm formation and virulence in *Burkholderia*
467 *cenocepacia*. *Infect Immun* **76**, 1979-1991.

468

469 Aubert, D. F., O'Grady, E. P., Hamad, M. A., Sokol, P. A. & Valvano, M. A. (2013).
470 The *Burkholderia cenocepacia* sensor kinase hybrid AtsR is a global regulator
471 modulating quorum-sensing signalling. *Environ Microbiol* **15**, 372-385.

472

473 Basler, M., Pilhofer, M., Henderson, G. P., Jensen, G. J. & Mekalanos, J. J. (2012).
474 Type VI secretion requires a dynamic contractile phage tail-like structure. *Nature* **483**,
475 182-186.

476

477 Bonemann, G., Pietrosiuk, A., Diemand, A., Zentgraf, H. & Mogk, A. (2009).
478 Remodelling of VipA/VipB tubules by ClpV-mediated threading is crucial for type VI
479 protein secretion. *EMBO J* **28**, 315-325.

480

481 Bonemann, G., Pietrosiuk, A. & Mogk, A. (2010). Tubules and donuts: a type VI
482 secretion story. *Mol Microbiol* **76**, 815-821.

483

484 Boyer, F., Fichant, G., Berthod, J., Vandenbrouck, Y. & Attree, I. (2009). Dissecting
485 the bacterial type VI secretion system by a genome wide in silico analysis: what can be
486 learned from available microbial genomic resources? *BMC Genomics* **10**, 104.

487

488 Brooks, T. M., Unterweger, D., Bachmann, V., Kostiuk, B. & Pukatzki, S. (2013).
489 Lytic activity of the *Vibrio cholerae* type VI secretion toxin VgrG-3 is inhibited by the
490 antitoxin TsaB. *J Biol Chem* **288**, 7618-7625.

491

492 **Burns, J. L., Jonas, M., Chi, E. Y., Clark, D. K., Berger, A. & Griffith, A. (1996).**
493 Invasion of respiratory epithelial cells by *Burkholderia (Pseudomonas) cepacia*. *Infect*
494 *Immun* **64**, 4054-4059.
495

496 **Clemens, D. L., Ge, P., Lee, B. Y., Horwitz, M. A. & Zhou, Z. H. (2015).** Atomic
497 structure of T6SS reveals interlaced array essential to function. *Cell* **160**, 940-951.
498

499 **Cohen, S. N., Chang, A. C. & Hsu, L. (1972).** Nonchromosomal antibiotic resistance in
500 bacteria: genetic transformation of *Escherichia coli* by R-factor DNA. *Proc Natl Acad*
501 *Sci U S A* **69**, 2110-2114.
502

503 **Costa, T. R., Felisberto-Rodrigues, C., Meir, A., Prevost, M. S., Redzej, A., Trokter,**
504 **M. & Waksman, G. (2015).** Secretion systems in Gram-negative bacteria: structural and
505 mechanistic insights. *Nat Rev Microbiol* **13**, 343-359.
506

507 **Cox, G. W., Mathieson, B. J., Gandino, L., Blasi, E., Radzioch, D. & Varesio, L.**
508 **(1989).** Heterogeneity of hematopoietic cells immortalized by v-myc/v-raf recombinant
509 retrovirus infection of bone marrow or fetal liver. *J Natl Cancer Inst* **81**, 1492-1496.
510

511 **Craig, F. F., Coote, J. G., Parton, R., Freer, J. H. & Gilmour, N. J. (1989).** A plasmid
512 which can be transferred between *Escherichia coli* and *Pasteurella haemolytica* by
513 electroporation and conjugation. *J Gen Microbiol* **135**, 2885-2890.
514

515 **Drevinek, P. & Mahenthiralingam, E. (2010).** *Burkholderia cenocepacia* in cystic
516 fibrosis: epidemiology and molecular mechanisms of virulence. *Clin Microbiol Infect* **16**,
517 821-830.
518

519 **Durand, E., Zoued, A., Spinelli, S., Watson, P. J., Aschtgen, M. S., Journet, L.,**
520 **Cambillau, C. & Cascales, E. (2012).** Structural characterization and oligomerization of
521 the TssL protein, a component shared by bacterial type VI and type IVb secretion
522 systems. *J Biol Chem* **287**, 14157-14168.
523

524 **Durand, E., Cambillau, C., Cascales, E. & Journet, L. (2014).** VgrG, Tae, Tle, and
525 beyond: the versatile arsenal of Type VI secretion effectors. *Trends Microbiol* **22**, 498-
526 507.
527

528 **English, G., Byron, O., Cianfanelli, F. R., Prescott, A. R. & Coulthurst, S. J. (2014).**
529 Biochemical analysis of TssK, a core component of the bacterial Type VI secretion
530 system, reveals distinct oligomeric states of TssK and identifies a TssK-TssFG
531 subcomplex. *Biochem J* **461**, 291-304.
532

533 **Felisberto-Rodrigues, C., Durand, E., Aschtgen, M. S., Blangy, S., Ortiz-Lombardia,**
534 **M., Douzi, B., Cambillau, C. & Cascales, E. (2011).** Towards a structural
535 comprehension of bacterial type VI secretion systems: characterization of the TssJ-TssM
536 complex of an *Escherichia coli* pathovar. *PLoS Pathog* **7**, e1002386.
537

538 **Figurski, D. H. & Helinski, D. R. (1979).** Replication of an origin-containing derivative
539 of plasmid RK2 dependent on a plasmid function provided in *trans*. *Proc Natl Acad Sci*
540 *USA* **76**, 1648-1652.
541

542 **Flannagan, R. S., Linn, T. & Valvano, M. A. (2008).** A system for the construction of
543 targeted unmarked gene deletions in the genus *Burkholderia*. *Environ Microbiol* **10**,
544 1652-1660.
545

546 **Flannagan, R. S., Jaumouillé, V., Huynh, K. K., Plumb, J. D., Downey, G. P.,**
547 **Valvano, M. A. & Grinstein, S. (2012).** *Burkholderia cenocepacia* disrupts host cell
548 actin cytoskeleton by inactivating Rac and Cdc42. *Cell Microbiol* **14**, 239-254.
549

550 **Hamad, M. A., Skeldon, A. M. & Valvano, M. A. (2010).** Construction of
551 aminoglycoside-sensitive *Burkholderia cenocepacia* strains for use in studies of
552 intracellular bacteria with the gentamicin protection assay. *Appl Environ Microbiol* **76**,
553 3170-3176.
554

555 **Hunt, T. A., Kooi, C., Sokol, P. A. & Valvano, M. A. (2004).** Identification of
556 *Burkholderia cenocepacia* (formerly *Burkholderia cepacia* genomovar III) genes
557 required for bacterial survival in vivo. *Infect Immun* **72**, 4010-4022.
558

559 **Isles, A., Maclusky, I., Corey, M., Gold, R., Prober, C., Fleming, P. & Levison, H.**
560 **(1984).** *Pseudomonas cepacia* infection in cystic fibrosis: an emerging problem. *J*
561 *Pediatr* **104**, 206-210.
562

563 **Jiang, F., Waterfield, N. R., Yang, J., Yang, G. & Jin, Q. (2014).** A *Pseudomonas*
564 *aeruginosa* Type VI Secretion Phospholipase D Effector Targets Both Prokaryotic and
565 Eukaryotic Cells. *Cell Host Microbe* **15**, 600-610.
566

567 **Kanehisa, M. & Goto, S. (2000).** KEGG: kyoto encyclopedia of genes and genomes.
568 *Nucleic Acids Res* **28**, 27-30.
569

570 **Keith, K. E., Hynes, D. W., Sholdice, J. E. & Valvano, M. A. (2009).** Delayed
571 association of the NADPH oxidase complex with macrophage vacuoles containing the
572 opportunistic pathogen *Burkholderia cenocepacia*. *Microbiology* **155**, 1004-1015.
573

574 **Khodai-Kalaki, M., Aubert, D. F. & Valvano, M. A. (2013).** Characterization of the
575 AtsR hybrid sensor kinase phosphorelay pathway and identification of its response
576 regulator in *Burkholderia cenocepacia*. *J Biol Chem* **288**, 30473-30484.
577

578 **Khodai-Kalaki, M., Andrade, A., Fathy Mohamed, Y. & Valvano, M. A. (2015).**
579 *Burkholderia cenocepacia* lipopolysaccharide modification and flagellin glycosylation
580 affect virulence but not innate immune recognition in plants. *MBio* **6**.
581

582 **Kudryashev, M., Wang, R. Y., Brackmann, M. & other authors (2015).** Structure of
583 the type VI secretion system contractile sheath. *Cell* **160**, 952-962.

584
585 **Lamothe, J., Thyssen, S. & Valvano, M. A. (2004).** *Burkholderia cepacia* complex
586 isolates survive intracellularly without replication within acidic vacuoles of
587 *Acanthamoeba polyphaga*. *Cell Microbiol* **6**, 1127-1138.
588
589 **Lamothe, J., Huynh, K. K., Grinstein, S. & Valvano, M. A. (2007).** Intracellular
590 survival of *Burkholderia cenocepacia* in macrophages is associated with a delay in the
591 maturation of bacteria-containing vacuoles. *Cell Microbiol* **9**, 40-53.
592
593 **Mahenthiralingam, E., Coenye, T., Chung, J. W., Speert, D. P., Govan, J. R.,**
594 **Taylor, P. & Vandamme, P. (2000).** Diagnostically and experimentally useful panel of
595 strains from the *Burkholderia cepacia* complex. *J Clin Microbiol* **38**, 910-913.
596
597 **Mahenthiralingam, E., Baldwin, A. & Dowson, C. G. (2008).** *Burkholderia cepacia*
598 complex bacteria: opportunistic pathogens with important natural biology. *J Appl*
599 *Microbiol* **104**, 1539-1551.
600
601 **Marolda, C. L., Hauröder, B., John, M. A., Michel, R. & Valvano, M. A. (1999).**
602 Intracellular survival and saprophytic growth of isolates from the *Burkholderia cepacia*
603 Complex in free-living amoebae. *Microbiology* **145**, 1509-1517.
604
605 **Martin, D. W. & Mohr, C. D. (2000).** Invasion and intracellular survival of
606 *Burkholderia cepacia*. *Infect Immun* **68**, 24-29.
607
608 **Pukatzki, S., Ma, A. T., Revel, A. T., Sturtevant, D. & Mekalanos, J. J. (2007).** Type
609 VI secretion system translocates a phage tail spike-like protein into target cells where it
610 cross-links actin. *Proc Natl Acad Sci U S A* **104**, 15508-15513.
611
612 **Rosales-Reyes, R., Skeldon, A. M., Aubert, D. F. & Valvano, M. A. (2012).** The Type
613 VI secretion system of *Burkholderia cenocepacia* targets multiple Rho family GTPases
614 disrupting the actin cytoskeleton and the assembly of NADPH oxidase complex in
615 macrophages. *Cell Microbiol* **14**, 255-273.
616
617 **Russell, A. B., Hood, R. D., Bui, N. K., LeRoux, M., Vollmer, W. & Mougous, J. D.**
618 **(2011).** Type VI secretion delivers bacteriolytic effectors to target cells. *Nature* **475**, 343-
619 347.
620
621 **Russell, A. B., Peterson, S. B. & Mougous, J. D. (2014).** Type VI secretion system
622 effectors: poisons with a purpose. *Nat Rev Microbiol* **12**, 137-148.
623
624 **Saini, L., Galsworthy, S., John, M. & Valvano, M. A. (1999).** Intracellular survival of
625 *Burkholderia cepacia* complex isolates in the presence of macrophage cell activation.
626 *Microbiology* **145**, 3465-3475.
627

628 **Sajjan, U. S., Yang, J. H., Hershenson, M. B. & LiPuma, J. J. (2006).** Intracellular
629 trafficking and replication of *Burkholderia cenocepacia* in human cystic fibrosis airway
630 epithelial cells. *Cell Microbiol* **8**, 1456-1466.
631

632 **Sambrook, J., Fritsch, E. F. & Maniatis, T. (1990).** *Molecular cloning: a laboratory*
633 *manual*, 2nd edn. Cold Spring Harbor, New York: Cold Spring Harbor Laboratory.
634

635 **Schmerk, C. L. & Valvano, M. A. (2013).** *Burkholderia multivorans* survival and
636 trafficking within macrophages. *J Med Microbiol* **62**, 173-184.
637

638 **Schwarz, S., Singh, P., Robertson, J. D., LeRoux, M., Skerrett, S. J., Goodlett, D. R.,**
639 **West, T. E. & Mougous, J. D. (2014).** VgrG-5 is a *Burkholderia* type VI secretion
640 system-exported protein required for multinucleated giant cell formation and virulence.
641 *Infect Immun* **82**, 1445-1452.
642

643 **Shalom, G., Shaw, J. G. & Thomas, M. S. (2007).** *In vivo* expression technology
644 identifies a type VI secretion system locus in *Burkholderia pseudomallei* that is induced
645 upon invasion of macrophages. *Microbiology* **153**, 2689-2699.
646

647 **Shneider, M. M., Buth, S. A., Ho, B. T., Basler, M., Mekalanos, J. J. & Leiman, P.**
648 **G. (2013).** PAAR-repeat proteins sharpen and diversify the type VI secretion system
649 spike. *Nature* **500**, 350-353.
650

651 **Smith, T. F. & Waterman, M. S. (1981).** Identification of common molecular
652 subsequences. *J Mol Biol* **147**, 195-197.
653

654 **Suarez, G., Sierra, J. C., Erova, T. E., Sha, J., Horneman, A. J. & Chopra, A. K.**
655 **(2010).** A type VI secretion system effector protein, VgrG1, from *Aeromonas hydrophila*
656 that induces host cell toxicity by ADP ribosylation of actin. *J Bacteriol* **192**, 155-168.
657

658 **Thomson, E. L. S. & Dennis, J. J. (2013).** Common Duckweed (*Lemna minor*) Is a
659 Versatile High-Throughput Infection Model For the *Burkholderia cepacia* Complex and
660 Other Pathogenic Bacteria. *Plos One* **8**.
661

662 **Toesca, I. J., French, C. T. & Miller, J. F. (2014).** The Type VI secretion system spike
663 protein VgrG5 mediates membrane fusion during intercellular spread by pseudomallei
664 group *Burkholderia* species. *Infect Immun* **82**, 1436-1444.
665

666 **Uehlinger, S., Schwager, S., Bernier, S. P., Riedel, K., Nguyen, D. T., Sokol, P. A. &**
667 **Eberl, L. (2009).** Identification of Specific and Universal Virulence Factors in
668 *Burkholderia cenocepacia* Strains by Using Multiple Infection Hosts. *Infection and*
669 *Immunity* **77**, 4102-4110.
670

671 **Varga, J. J., Losada, L., Zelazny, A. M. & other authors (2013).** Draft Genome
672 Sequences of *Burkholderia cenocepacia* ET12 Lineage Strains K56-2 and BC7. *Genome*
673 *Announc* **1**.

674

675 **Vergunst, A. C., Meijer, A. H., Renshaw, S. A. & O'Callaghan, D. (2010).**
676 *Burkholderia cenocepacia* creates an intramacrophage replication niche in zebrafish
677 embryos, followed by bacterial dissemination and establishment of systemic infection.
678 *Infect Immun* **78**, 1495-1508.

679

680 **Waters, V. (2012).** New treatments for emerging cystic fibrosis pathogens other than
681 *Pseudomonas*. *Curr Pharm Des* **18**, 696-725.

682

683 **Zheng, J. & Leung, K. Y. (2007).** Dissection of a type VI secretion system in
684 *Edwardsiella tarda*. *Mol Microbiol* **66**, 1192-1206.

685

686 **Zheng, J., Ho, B. & Mekalanos, J. J. (2011).** Genetic analysis of anti-amoebae and anti-
687 bacterial activities of the type VI secretion system in *Vibrio cholerae*. *PLoS One* **6**,
688 e23876.

689

690 **Zoued, A., Durand, E., Bebeacua, C., Brunet, Y. R., Douzi, B., Cambillau, C.,**
691 **Cascales, E. & Journet, L. (2013).** TssK is a trimeric cytoplasmic protein interacting
692 with components of both phage-like and membrane anchoring complexes of the type VI
693 secretion system. *J Biol Chem* **288**, 27031-27041.

694

695 **Zoued, A., Brunet, Y. R., Durand, E., Aschtgen, M. S., Logger, L., Douzi, B.,**
696 **Journet, L., Cambillau, C. & Cascales, E. (2014).** Architecture and assembly of the
697 Type VI secretion system. *Biochim Biophys Acta*.

698

699

700

701

702

703

704

Table 1. Strains and plasmids

705

706

707

708

709

710

711

712

713

714

715

716

717

718

719

720

721

722

723

724

725

726

727

728

729

730

731

732

733

734

735

736

737

738

739

740

741

742

743

744

745

746

747

748

749

750

751

752

753

754

755

756

757

758

759

Strain or plasmid	Relevant characteristics ^a	Source and/or reference
<i>B. cenocepacia</i>		
K56-2	ET12 clone related to J2315, CF clinical Isolate	^b BCRRC, (Mahenthiralingam <i>et al.</i> , 2000)
2000)		
K56-2 Δ atsR	Deletion of <i>atsR</i> in K56-2	(Aubert <i>et al.</i> , 2010)
K56-2 Δ atsR Gm ^S	Deletion of BCAL1674-76 in K56-2 Δ atsR - Gm ^S	This study
K56-2 Δ atsR Δ BCAL1165	Deletion of BCAL1165 in K56-2 Δ atsR	This study
K56-2 Δ atsR Δ BCAL1293	Deletion of BCAL1293 in K56-2 Δ atsR	This study
K56-2 Δ atsR Δ BCAL1294	Deletion of BCAL1294 in K56-2 Δ atsR	This study
K56-2 Δ atsR Δ BCAL1355	Deletion of BCAL1355 in K56-2 Δ atsR	This study
K56-2 Δ atsR Δ BCAL1359	Deletion of BCAL1359 in K56-2 Δ atsR	This study
K56-2 Δ atsR Δ BCAL1362	Deletion of BCAL1362 in K56-2 Δ atsR	This study
K56-2 Δ atsR Δ BCAL2279	Deletion of BCAL2279 in K56-2 Δ atsR	This study
K56-2 Δ atsR Δ BCAM0043	Deletion of BCAM0043 in K56-2 Δ atsR	This study
K56-2 Δ atsR Δ BCAM0148	Deletion of BCAM0148 in K56-2 Δ atsR	This study
K56-2 Δ atsR Δ BCAM2254	Deletion of BCAM2254 in K56-2 Δ atsR	This study
K56-2 Δ atsR Δ BCAS0667	Deletion of BCAS0667 in K56-2 Δ atsR	This study
K56-2 Δ atsR Δ BCAS0668	Deletion of BCAS0668 in K56-2 Δ atsR	This study
K56-2 Δ atsR Δ BCAL0352	Deletion of BCAL0352 in K56-2 Δ atsR	This study
K56-2 Δ atsR Δ BCAL0351	Deletion of BCAL0351 in K56-2 Δ atsR	This study
K56-2 Δ atsR Δ BCAL0350	Deletion of BCAL0350 in K56-2 Δ atsR	This study
K56-2 Δ atsR Δ BCAL0349	Deletion of BCAL0349 in K56-2 Δ atsR	This study
K56-2 Δ atsR Δ BCAL0348	Deletion of BCAL0348 (<i>bcsE</i>) in K56-2 Δ atsR	(Aubert <i>et al.</i> , 2010)
K56-2 Δ atsR Δ BCAL0347	Deletion of BCAL0347 (<i>bcsF</i>) in K56-2 Δ atsR	(Aubert <i>et al.</i> , 2010)
K56-2 Δ atsR Δ BCAL0346	Deletion of BCAL0346 (<i>bcsG</i>) in K56-2 Δ atsR	(Aubert <i>et al.</i> , 2010)
K56-2 Δ atsR Δ BCAL0345	Deletion of BCAL0345 (<i>bcsH</i>) in K56-2 Δ atsR	(Aubert <i>et al.</i> , 2010)
K56-2 Δ atsR Δ BCAL0344	Deletion of BCAL0344 (<i>bcsI</i>) in K56-2 Δ atsR	(Aubert <i>et al.</i> , 2010)
K56-2 Δ atsR Δ hcp	Deletion of BCAL0343 in K56-2 Δ atsR	(Aubert <i>et al.</i> , 2010)
K56-2 Δ atsR Δ BCAL0342	Deletion of BCAL0342 (<i>bcsK</i>) in K56-2 Δ atsR	(Aubert <i>et al.</i> , 2010)
K56-2 Δ atsR Δ BCAL0341	Deletion of BCAL0341 (<i>bcsL</i>) in K56-2 Δ atsR	(Aubert <i>et al.</i> , 2010)
K56-2 Δ atsR Δ BCAL0340	Deletion of BCAL0340 (<i>bcsM</i>) in K56-2 Δ atsR	(Aubert <i>et al.</i> , 2010)
K56-2 Δ atsR Δ BCAL0339	Deletion of BCAL0339 in K56-2 Δ atsR	This study
K56-2 Δ atsR Δ BCAL0338	Deletion of BCAL0338 in K56-2 Δ atsR	This study
K56-2 Δ atsR Δ BCAL0339	Deletion of BCAL0337 in K56-2 Δ atsR	This study
K56-2 Δ atsR Δ BCAL0336-33	Deletion of BCAL0336-0333 in K56-2 Δ atsR	This study
K56-2 Δ atsR Δ 10vgrGs	Deletion of BCAL1165, 1294, 1355, 1359, 1362, 2279, BCAM0043, 0148, 2254 and BCAS0667 in K56-2 Δ atsR - VgrG-less strain	This study
<i>E. coli</i>		
BL21 (DE3)	F ⁻ <i>ompT hsdSB</i> (r _B ⁻ m _B ⁻) <i>gal dcm</i> (λ DE3)	Laboratory stock
DH5 α	F ϕ 80 <i>lacZ</i> M15 <i>endA1 recA1 supE44 hsdR17</i> (r _K ⁻ m _K ⁺) <i>deoR thi-1 nupG supE44 gyrA96 relA1</i> Δ (<i>lacZYA-argF</i>)U169, λ -	Laboratory stock
GT115	F ⁻ <i>mcrA</i> Δ (<i>mrr-hsdRMS-mcrBC</i>) ϕ 80 <i>lacZ</i> Δ M15 Δ <i>lacX74 recA1 rpsL</i> (StrA) <i>endA1</i> Δ <i>dcm uidA</i> (Δ MluI):: <i>pir-116</i> Δ <i>sbcC-sbcD</i>	Invivogen
Plasmids		
pL0345	BCAL0345 cloned into pDA12	This study
pL1293	BCAL1293 cloned into pDA12	This study
pS0668	BCAS0668 cloned into pDA12	This study
pDA12	cloning vector, <i>ori</i> _{pBBR1} , Tet ^R , <i>mob</i> ⁺ , <i>P_{dhfr}</i>	(Aubert <i>et al.</i> , 2008)
pDA44	<i>hcp</i> _{6xHis} cloned into pET30a	This study

760	pDAI-SceI-SacB	<i>ori</i> _{pBBR1} , Tet ^R , <i>P_{dhfr}</i> , <i>mob</i> ⁺ , expressing I-SceI, SacB	(Hamad <i>et al.</i> , 2010)
761	pDelL0352	pGPI-SceI with fragments flanking BCAL0352	This study
762	pDelL0351	pGPI-SceI with fragments flanking BCAL0351	This study
763	pDelL0350	pGPI-SceI with fragments flanking BCAL0350	This study
764	pDelL0349	pGPI-SceI with fragments flanking BCAL0349	This study
765	pDelL0339	pGPI-SceI with fragments flanking BCAL0339	This study
766	pDelL0338	pGPI-SceI with fragments flanking BCAL0338	This study
767	pDelL0337	pGPI-SceI with fragments flanking BCAL0337	This study
768	pDelL0036-33	pGPI-SceI with fragments flanking BCAL0336-0333	This study
769	pDelL1165	pGPI-SceI with fragments flanking BCAL1165	This study
770	pDelL1293	pGPI-SceI with fragments flanking BCAL1293	This study
771	pDelL1294	pGPI-SceI with fragments flanking BCAL1294	This study
772	pDelL1355	pGPI-SceI with fragments flanking BCAL1355	This study
773	pDelL1359	pGPI-SceI with fragments flanking BCAL1359	This study
774	pDelL1362	pGPI-SceI with fragments flanking BCAL1362	This study
775	pDelL2279	pGPI-SceI with fragments flanking BCAL2279	This study
776	pDelM0043	pGPI-SceI with fragments flanking BCAM0043	This study
777	pDelM0148	pGPI-SceI with fragments flanking BCAM0148	This study
778	pDelM1857	pGPI-SceI with fragments flanking BCAM1857	This study
779	pDelM2254	pGPI-SceI with fragments flanking BCAM2254	This study
780	pDelS0667	pGPI-SceI with fragments flanking BCAS0667	This study
781	pDelS0668	pGPI-SceI with fragments flanking BCAS0668	This study
782	pET30a	Expression vector, Kan ^R	Novagen
783	pGPI-SceI	<i>ori</i> _{R6K} , □Tp ^R , <i>mob</i> ⁺ , including an I-SceI restriction site	(Flannagan <i>et al.</i> , 2008)
784	pMH447	pGPI-SceI with fragments flanking BCAL1674-1676	(Hamad <i>et al.</i> , 2010)
785	pRK2013	<i>ori</i> _{colEI} , RK2 derivative, Kan ^R , <i>mob</i> ⁺ , <i>tra</i> ⁺	(Figurski & Helinski, 1979)
786			
787	^a Gm ^S , gentamicin sensitive, Kan ^R , kanamycin resistance, Tet ^R , tetracycline resistance, Tp ^R , trimethoprim resistance.		
788	^b BCRRRC, <i>B. cepacia</i> Research and Referral Repository for Canadian CF Clinics.		

789

790 **FIGURE LEGENDS**

791

792 **Fig.1.** Investigation of the *B. cenocepacia* T6SS gene cluster. (a) Genetic map of the *B.*
793 *cenocepacia* K56-2 T6SS gene cluster. The arrows represent the location and direction of
794 transcription of each gene. The “BCAL” locus tags assigned by the Sanger Center are
795 shown above and the standard *tss* or *tag* annotation of the genes (listed in Supplemental
796 Table S2) is shown below. White, grey and black arrows represent the critical
797 components, accessory proteins and dispensable elements for T6SS activity identified in
798 this study, respectively. The genes encoding the well-characterized components IcmF
799 (BCAL0351; TssM_{Bc}), ClpV (BCAL0347; TssH_{Bc}), and Hcp (BCAL0343; TssD_{Bc}) and
800 location of the tRNA threonine (tRNA-Thr) sequence are shown. (b) Phase-contrast
801 microscopy of infected ANA-1 macrophages and qualitative assessment of T6SS activity.
802 The infections were performed at an MOI of 50:1 for 4 h. The presence of ectopic
803 structures is indicative of expression and functionality of the T6SS. Characteristic ‘beads’
804 surrounding infected macrophages are shown by white arrows. Infections were repeated
805 independently and reproducible results were obtained. The pictures shown are
806 representatives. (c) Measurement of T6SS activity. The proportion of dark “beads on a
807 string-like” structures around macrophages was measured using image analysis software.
808 Results were expressed in arbitrary units relative to Δ *atsR* set as 1 (white bar). Values are
809 mean \pm standard deviation for at least 21 fields of view and are representative of three
810 independent experiments. Uninfected cells were used as negative control to determine the
811 background level. The dotted line indicates the 0.2 relative units threshold indicative of
812 no “beads on a string-like” structures. ***, $p < 0.001$ compared to the relative units of

813 uninfected cells (see Methods for details on the statistical analysis). (d) Western blot
814 analysis of total cell lysates (Pellet) and concentrated culture supernatants recovered from
815 $\Delta atsR$ and T6SS mutants using anti-RNAP α subunit (cytosolic protein, cell lysis control)
816 and anti-Hcp antibodies. The upper band seen in the pellet fractions with the anti-Hcp
817 antibody corresponds to a cross-reacting unspecific protein.

818

819 **Fig.2.** Investigation of the *tssF* (BCAL0345) paralogs. Phase-contrast microscopy of
820 infected ANA-1 macrophages and qualitative assessment of T6SS activity. The infections
821 were performed at an MOI of 50:1 for 4 h with *B. cenocepacia* K56-2 $\Delta atsR$, derivative
822 mutants in *tssF* or paralogs (BCAL1293 and BCAS0668) and mutants carrying plasmids
823 pL0345, pL1293 or pS0668, which express TssF, BCAL1293 and BCAS0668,
824 respectively. Formation of ectopic structures indicates T6SS functionality. Infections
825 were repeated independently and reproducible results were obtained. The pictures shown
826 are representatives.

827

828 **Fig. 3.** Putative conserved domains detected within the VgrGs of *B. cenocepacia* K56-2.
829 Conserved domains within VgrGs were detected using PFAM search
830 (<http://pfam.sanger.ac.uk>). The VgrG2 (VCA0018) from *Vibrio cholerae* was used as
831 query to identify the VgrGs from *B. cenocepacia* K56-2 and is shown here for
832 comparison. Domains are as follows: Phage_GPD (green), Phage_base_V (red),
833 T6SS_Vgr (blue), DUF2345 (yellow). The putative effector domains found at the C-
834 terminus of BCAL1359 and BCAS0667 are represented with a grey (M6 family
835 metalloprotease domain) and brown (lipase_3 domain) circle, respectively.

836

837 **Fig. 4.** Investigation of the *B. cenocepacia* VgrGs. (a) Measurement of T6SS activity.
838 The infections were performed at an MOI of 50:1 for 4 h with *B. cenocepacia* K56-2
839 Δ *atsR* and derivative *vgrG* mutants. The proportion of dark “beads on a string-like”
840 structures around macrophages was measured as described in Methods and in the Fig. 1
841 legend. The dotted line indicates the 0.2 relative units threshold indicative of no “beads
842 on a string-like” structures. All the single *vgrG* deletion strains induced “beads on a
843 string-like” structures at a similar level as Δ *atsR* (no statistically significant differences)
844 and significantly different levels ($p < 0.001$) from uninfected cells. (b) and (c) Western
845 blot analysis of total cell lysates (Pellet) and concentrated culture supernatants recovered
846 from *B. cenocepacia* K56-2 Δ *atsR*, Δ *atsR* Δ *hcp*, *vgrG* mutants and from the *vgrG*-less
847 strain K56-2 Δ *atsR* Δ 10*vgrGs* using anti-RNAP α subunit (cytosolic protein, cell lysis
848 control) and anti-Hcp antibodies.

849

Figure 1 BCAL0352 - BCAL0333
[Click here to download Figure: Aubert_T6SSactivity_m-Fig1-revised.eps](#)

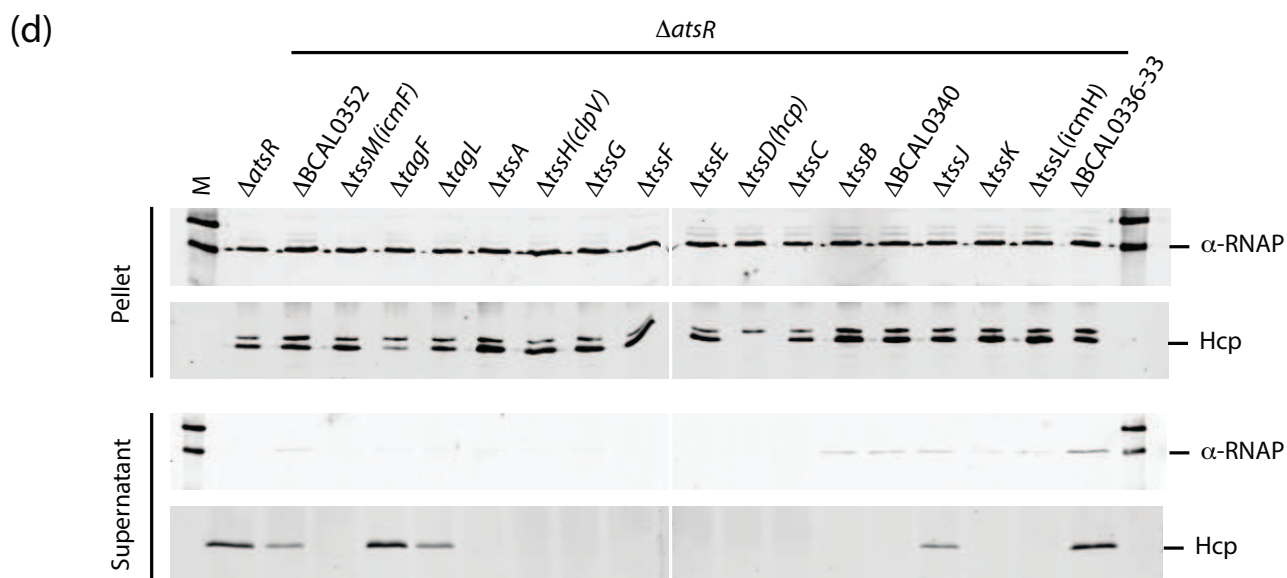
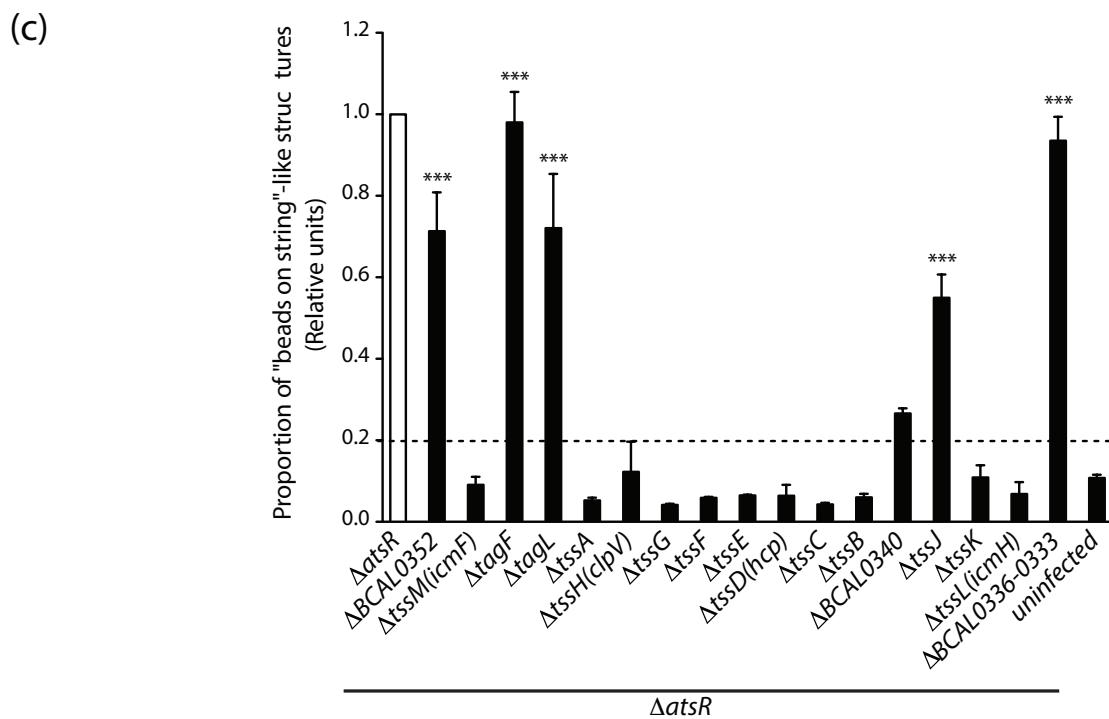
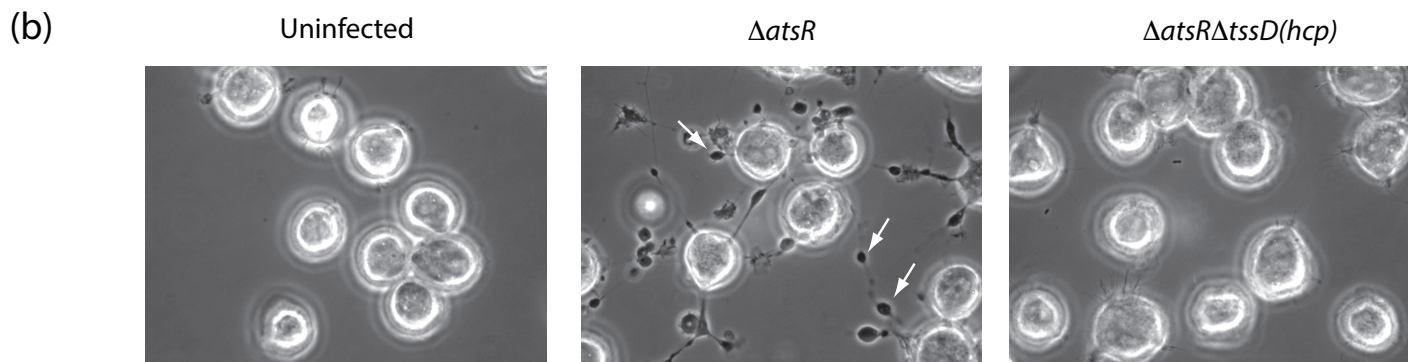
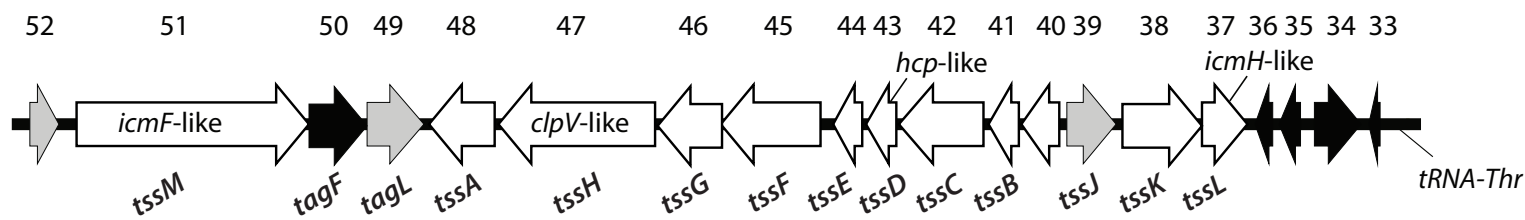
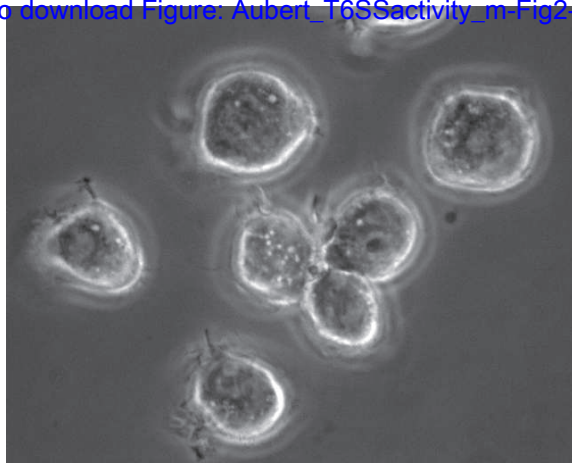


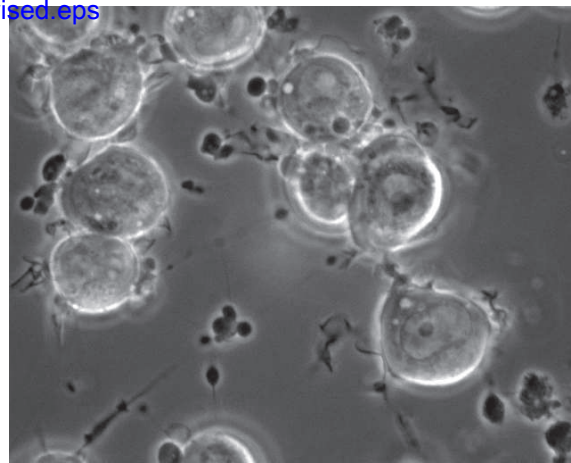
Figure 2

[Click here to download Figure: Aubert_T6SSactivity_m-Fig2-revised.eps](#)

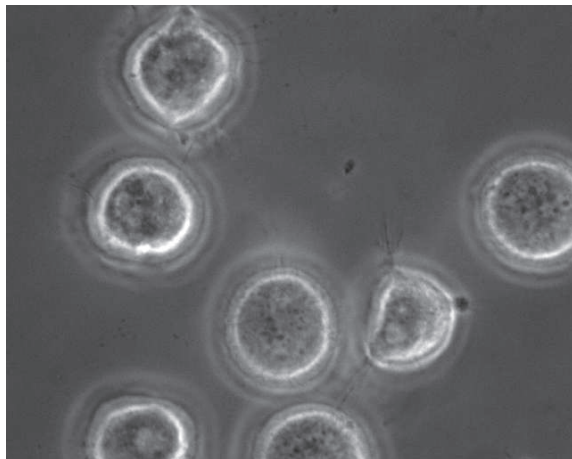
Uninfected



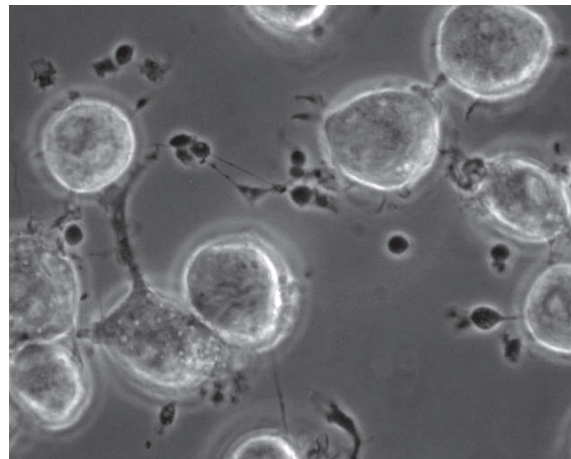
$\Delta atsR$



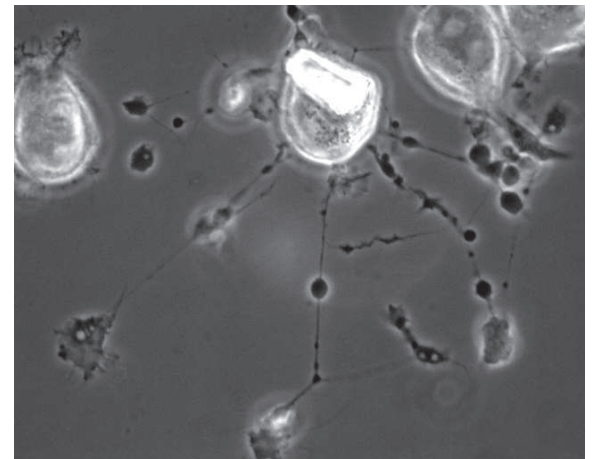
$\Delta atsR \Delta tssF$



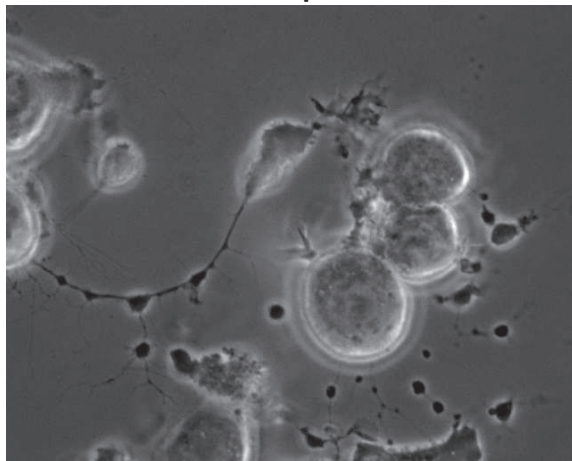
$\Delta atsR \Delta BCAL1293$



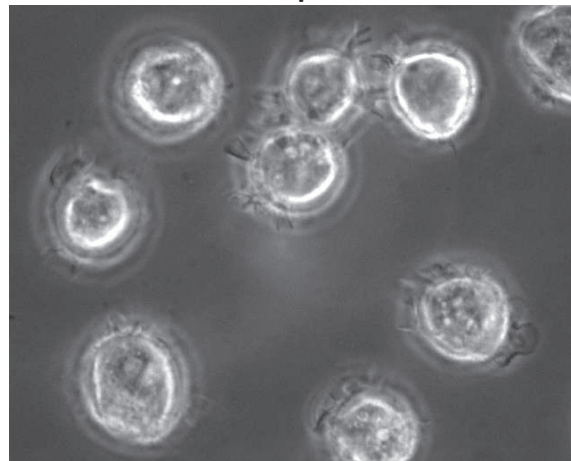
$\Delta atsR \Delta BCAS0668$



$\Delta atsR \Delta tssF$ pL0345(TssF)



$\Delta atsR \Delta tssF$ pL1293



$\Delta atsR \Delta tssF$ pS0668

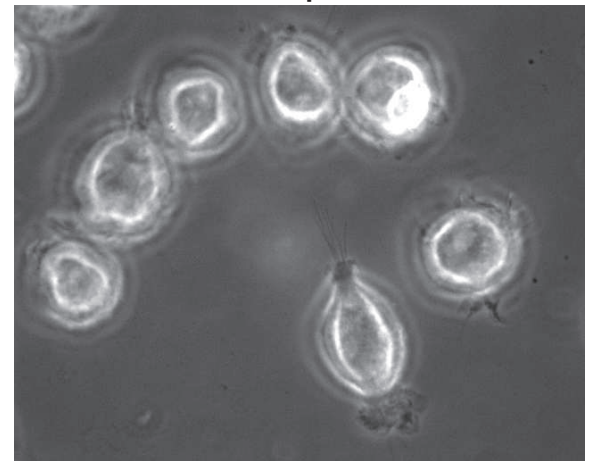


Figure 3

[Click here to download Figure: Aubert_T6SSActivity_m-Fig3-revised.eps](#)

VCA0018



BCAL1165



BCAL1294



BCAL1355



BCAL1359



BCAL1362



BCAL2279



BCAM0043



BCAM0148



BCAM2254



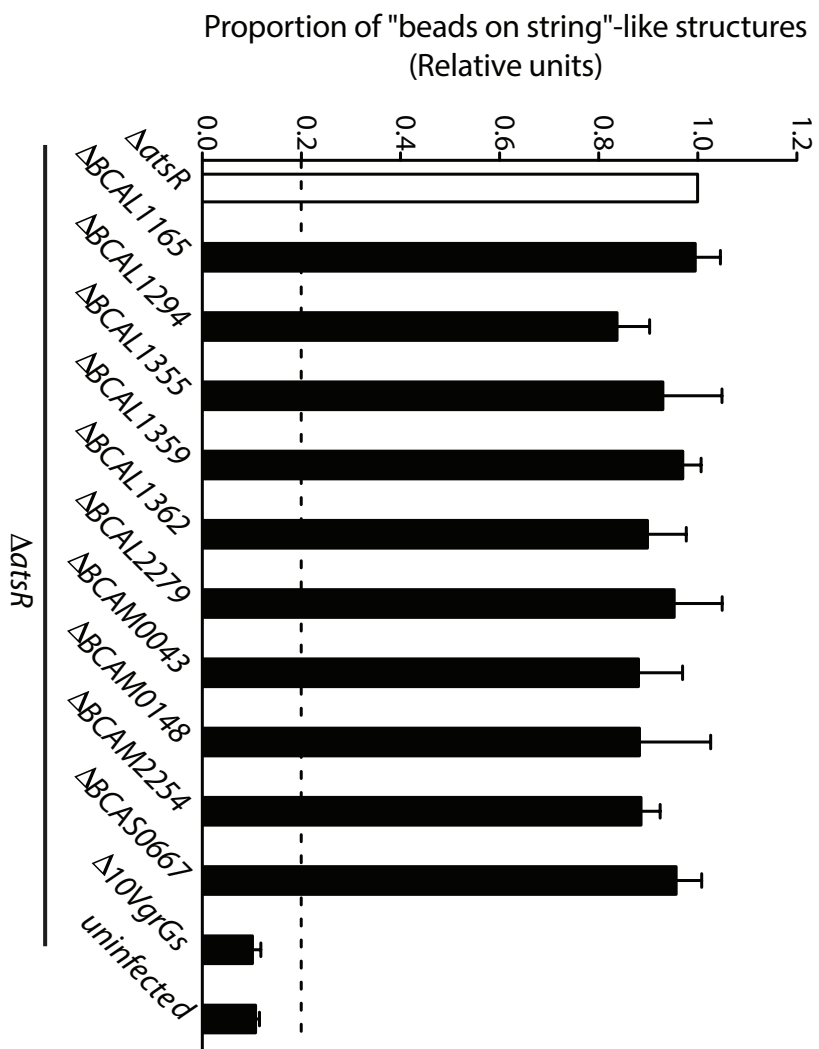
BCAS0667



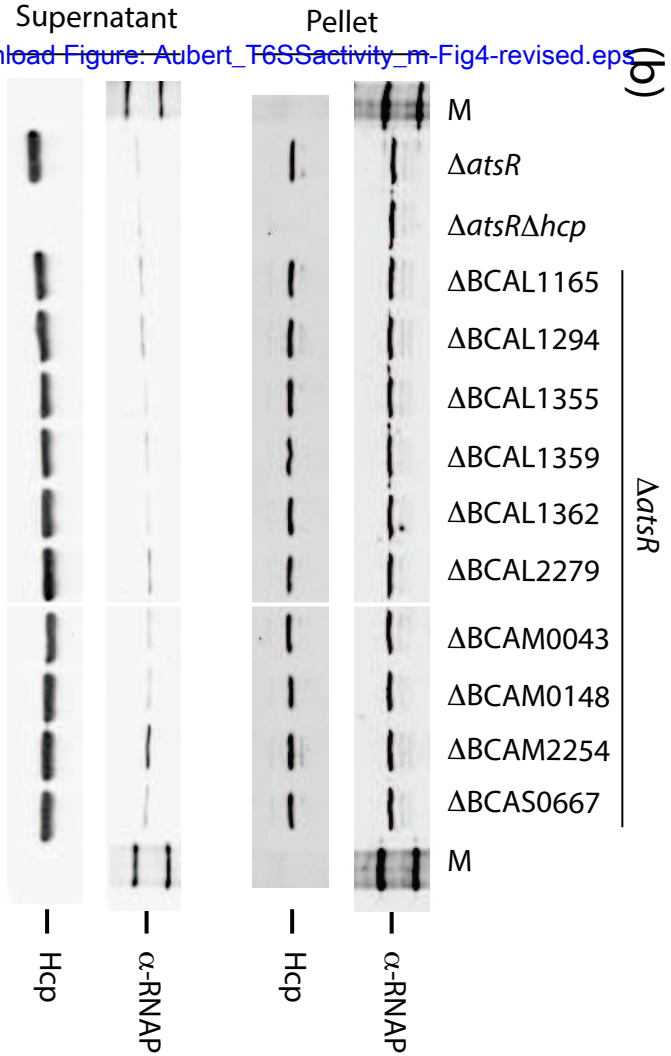
Figure 4

[Click here to download Figure: Aubert_T6SSActivity_m-Fig4-revised.eps](#)

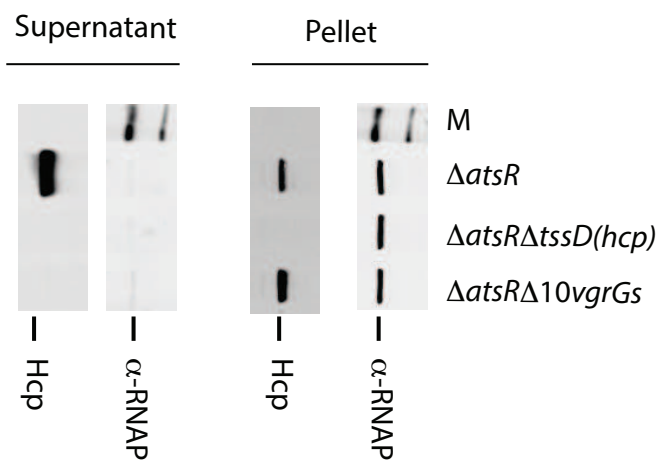
(a)



(b)



(c)



SUPPLEMENTAL DATA

**Quantification of Type VI secretion system activity in macrophages infected with
*Burkholderia cenocepacia***

Daniel F. Aubert¹, Sherry Hu¹ and Miguel A. Valvano^{1,2}

¹Department of Microbiology and Immunology, University of Western Ontario, London,
Ontario N6A 5C1, Canada;

²Centre for Infection and Immunity, Queen's University Belfast, BT9 5GZ, Belfast,
United Kingdom

Table S1

Oligonucleotide primers

Primer No.	5'-3' Primer sequence	Restriction enzyme*
430	TGTGGCTGCACTTGAACG	N/A
2143	AGTCGAAGGCATATGTTACACATGCACTTGCAG	NdeI
2748	TCGAAAGCTTGACCGCGTAGGTCTTGTCGT	HindIII
2863	TTTACCCGGGTCTTGACAGGGACGATTTC	SmaI
2867	TACGTCTAGAATGAGCTCAAGCGGCTGT	XbaI
3059	TTTTTCTAGAAGATACGCAACGGCGATAAC	XbaI
3065	TTTTCTCGAGATTGCTCTGGAGCTGGAAGA	XhoI
3066	TTTTCTCGAGATTGAGTTGCGAACCGGTAA	XhoI
3068	TTTTGAATTCGCAGTCCTTTGTCGATGACC	EcoRI
3077	TAGGTACCATTCAACAAGAAGGATTCGA	KpnI
3080	TAGGTACCTTAGGCCACACGTTCAAG	KpnI
3177	TTAACTCGAGCGACGTCTTGATCGTCTTCA	XhoI
3201	GCTACGGTCTCGAGAAGCTG	XhoI
3202	AAAAGAATTCAGCCGAGAAACGCGAAAT	EcoRI
3203	TTTTTCTAGAATCTCACAGCGTCCTTTCGT	XbaI
3263	TTTACTCGAGTCGATGGTGAGAGCGTGAC	XhoI
3267	ATTACTCGAGATTCGGGGCGAAACTCAT	XhoI
3349	TTTATCTAGAAGGACGATGAAGGGTTTGGT	XbaI
3354	TAATCTCGAGATTGAATGCGCCAAAAGAG	XhoI
3454	TTTTTCTAGAGGCGACGATGAACAGAATG	XbaI
3457	TTTTGAATTCGCCGGTTTAGTATCGGACAG	EcoRI
3458	TTTTCTCGAGCGTGTGTCGTACTIONGGAACA	XhoI
3465	TTTTCTCGAGTACCAGTTGTACGGCCAGGT	XhoI
3759	TTTTTCTAGACGTCGCCTCTCTATTGCTCT	XbaI
3760	TTTTGCGGCCGCATGCGGGATCAAGACGTTAC	NotI
3761	AAAAGCGGCCGCGCGAATCAGGGGTTTCAGTA	NotI
3762	AAAAGAATTCCTCAAATACCCGCTCCTCATC	EcoRI
3800	AAAAGAATTCGTTGGCATGTGACTGTCTGG	EcoRI
3801	AAAACCTCGAGAGCTTAACCACGAAGCGAAA	XhoI
3947	TTTTTCTCGAGTAGCGAATCATGGACGATCT	XhoI
3948	TTTTTCTAGATGTTGAACACTTCCGCAGTC	XbaI
4125	TAATGAATTCCTCGTGTGATGAAATTGATG	EcoRI
4126	TAATGCGGCCGCAAAACGGGGTTCGAATGAAT	NotI
4127	TTTAGCGGCCGCGCGTCGCATACGTTTCATCG	NotI
4128	TTTTTCTAGAATCACGCTCTCCATCTGCTC	XbaI
4134	TTTTGAATTCCTGAGATCACACGCAAGGAA	EcoRI
4135	TTTTCTCGAGGACGTAGCCGTCGAAGTAGC	XhoI
4136	TTTTCTCGAGCTGGAAGCCAAGGACTIONCTG	XhoI
4137	TTTTTCTAGAAGGTGAGCATCAGGACAACC	XbaI
4185	AAAACCTCGAGGGTCAGTGTGCTCGACAAG	XhoI
4186	AAAATCTAGAATGCCAGCGCCTTCATATAG	XbaI
4305	TTTTGAATTCGCCGACTTCGAAAGAAAGTG	EcoRI
4306	TTTTGCGGCCGCTCAGCTGGTAGCAGGTCAAC	NotI
4308	TTTTGCGGCCGCAACCTGAGCCGAGTCTTCAA	NotI
4309	TTTTTCTAGAACC GCCCCAGTAATTCCTTCT	XbaI
4893	TTTTGAATTC AATTGCCGAGGTT CACAATC	EcoRI
4894	TTTTCTCGAGGCTACGTTCAACTCGTCGTG	XhoI

4895	TTTTCTCGAGCAAGCAGTCCGACTTCACGTT	XhoI
4896	TAATTCTAGATACATCGCAAACCACCATC	XbaI
4897	TTTTTTCATATGTGAATATTGCAGCGAATG	NdeI
4898	TTTTTCTAGACTATCTCCACTGACCTATAC	XbaI
4899	TTTTGAATTCCTTTATTTTCGTCTCAGG	EcoRI
4900	TTTTCTCGAGGCGTTCGTCCAAGGATTG	XhoI
4901	TTTTCTCGAGCGAGTGCTCACCTGACATTGC	XhoI
4902	TTTATCTAGAATGCCGAGAAGTTTCGAGAG	XbaI
4903	TATATTCATATGGCGTGACCGTCTGAAACG	NdeI
4904	TTTTTCTAGACTCTTCCGTCACCAGTCA	XbaI
4905	AAAAAACATATGGCAGGAAATATTGAGGTTC	NdeI
4906	AAAATCTAGAACTACGCCAGGATCGATTTC	XbaI
5015	TTATCTCGAGCAGTTTCCCGAAAAGGTCTG	XhoI
5016	TTATGAATTCGAGACGCACCAGAAATGCTT	EcoRI
5017	TTTTGAATTCCTGGAACCACAACCAGATCAA	EcoRI
5018	TTTTCTCGAGATGCGGCAACTAGATCCAT	XhoI
5019	TTTTCTCGAGACATCAACTCGCGACATCTG	XhoI
5020	TTTTTCTAGAGTACGTGCCCTCGTAATGGT	XbaI
5021	GAACTCGAATTCAGGCGATG	EcoRI
5022	TTTTCTCGAGACCTGCCATTCGATGAGGAT	XhoI
5023	TTTTCTCGAGGATGGAAGGCAACGACATC	XhoI
5024	TTTTTCTAGAAGTTTCGGCACGAGTTCATC	XbaI
5025	TTTTCTCGAGGCGCGTTTCATCATCGAC	XhoI
5026	TTTTTCTAGAAGATCGCGCACATGAAGG	XbaI
5177	TTTTGAATTCGTCGGGCAACGTATCCAGT	EcoRI
5178	TTTTCTCGAGTATGCTGTCTTCGGTCTCCTG	XhoI
5179	TTTTCTCGAGGTCGGGCAACGTATCCAGT	XhoI
5180	TTTTGAATTCATGCTGTCTTCGGTCTCCTG	EcoRI
5181	TTTTTCTAGAGATCCGCGTGCTGAACTC	XbaI
5182	TTTTCTCGAGGACGACGTCGACAAGCTC	XhoI
5183	TATAGAATTCGATCGACGACAAGACCGAGT	EcoRI
5184	TATACTCGAGAACCCGTCGTACAGCAAATC	XhoI
5185	TTTTTCTAGAACGTCAGCTGGTTCTTCCAC	XbaI
5186	TTTTCTCGAGGTACCTCGGGCTCAACACGTA	XhoI
5187	TTTTGAATTCATGGCACCTTCGACCTGAC	EcoRI
5188	TTTTCTCGAGGGCTTCGCATCCTCGTAGAC	XhoI
5189	TTTTCTCGAGCGTCAGCTACCTCGACCAACC	XhoI
5190	TTTTTCTAGAGTAGGTGTCGCGCAGCTTCT	XbaI
5191	TTTTGAATTCGTCAGCTACCTCGACCAACC	EcoRI
5192	TTTTCTCGAGGTAGGTGTCGCGCAGCTTCT	XhoI
5193	TTTTCTCGAGGGCAAGTTGATCCTCGACCAG	XhoI
5194	TTTTTCTAGAGGCTCGCTGTCGCATATT	XbaI
5333	TTTTGAATTCCTCGTGCTCAACATCAGCTTC	EcoRI
5334	TTTTCTCGAGCCGTAACCCTTTTTCGGATT	XhoI
6066	TTTTGAATTCACCGTACTCGACCCTTCCTT	EcoRI
5887	CTGTCATGCCATCCGTAAGA	N/A
6207	TTTTTTCATATGGAAAGGAGCTATCCGTGCAG	NdeI
6208	TTTTTCTAGACCTACAGGCGCGACAGAT	XbaI

*Restriction endonuclease sites incorporated in the oligonucleotide sequences are underlined.

N/A indicates absence of restriction site.

Table S2.**Annotation of T6SS cluster genes in *B. cenocepacia* K56-2**

BCAL Number	Standard Annotation^a	Predicted function^b
0352		Putative bacteriophage-like L-alanyl-D-glutamate peptidase; highly conserved in <i>Burkholderia</i> T6SSs (Boyer <i>et al.</i> , 2009).
0351	tssM	IcmF-like, inner membrane protein with a cytoplasmic region that has ATPase activity. It makes a complex with TssL and TagL (Felisberto-Rodrigues <i>et al.</i> , 2011).
0350	tagF	SciT domain, DUF2094, unknown function.
0349	tagL	OmpA-like peptidoglycan binding domain lipoprotein; PF0691 (Aschtgen <i>et al.</i> , 2010)
0348	tssA	Cytoplasmic protein (Cascales & Cambillau, 2012).
0347	tssH	ClpV-ATPase for the sheath assembly/disassembly (Bonemann <i>et al.</i> , 2009).
0346	tssG	Recruited to the membrane by TssK. (English <i>et al.</i> , 2014; Zoued <i>et al.</i> , 2013).
0345	tssF	Recruited to the membrane by TssK
0344	tssE	Similarity with the phage gp25 baseplate protein
0343	tssD	hcp-like, hexameric inner tube (Zoued <i>et al.</i> , 2014)
0342	tssC	Phage-like sheath subunit (Aubert <i>et al.</i> , 2010)
0341	tssB	Phage-like sheath subunit (Aubert <i>et al.</i> , 2010)
0340		Outer membrane lipoprotein, NlpI lipoprotein domain. Highly conserved in <i>Burkholderia</i> T6SSs (Boyer <i>et al.</i> , 2009)
0339	tssJ	Outer membrane lipoprotein (Felisberto-Rodrigues <i>et al.</i> , 2011).
0338	tssK	ImpJ, VasE trimeric complex interacts with TssF and TssG (English <i>et al.</i> , 2014; Zoued <i>et al.</i> , 2013).
0337	tssL	IcmH-like, dot U, inner membrane (Durand <i>et al.</i> , 2012).
0336		DUF4262, conserved in many bacterial and viral proteins. Not part of the <i>B. cenocepacia</i> T6SS (this work)
0335		Conserved hypothetical protein. Not part of the <i>B. cenocepacia</i>

	T6SS (this work)
0334	Putative amino-acid transporter periplasmic solute protein. Not part of the <i>B. cenocepacia</i> T6SS (this work)
0333	Putative "winged helix" DNA binding protein. Not part of the <i>B. cenocepacia</i> T6SS (this work)

^a Based on Shalom *et al.* (2007)

^b Based on BLASTP

(http://blast.ncbi.nlm.nih.gov/Blast.cgi?PROGRAM=blastp&PAGE_TYPE=BlastSearch&LINK_LOC=blasthome) and HHpred (<http://toolkit.tuebingen.mpg.de/hhpred>) searches.

SUPPLEMENTARY METHODS

Details of the construction of mutagenic and complementing plasmids

Mutagenesis of *B. cenocepacia* K56-2. Unmarked and non-polar deletions were performed as described previously (Flannagan *et al.*, 2008). Amplicons were digested with the appropriate restriction enzymes and cloned into plasmid pGPI-SceI (see below for details). Mobilization of mutagenesis plasmids into *Burkholderia* strains was performed by triparental mating using *E. coli* DH5 α carrying the helper plasmid pRK2013 (Craig *et al.*, 1989; Figurski & Helinski, 1979). Gene deletions were confirmed by PCR. Deletion of BCAL1674-76 was performed using plasmid pMH447 and resulted in K56-2 gentamicin sensitive strains.

Deletion of genes localized in the T6SS cluster. To delete BCAL0352, PCR amplifications of regions flanking BCAL0352 were performed using 3454-3465 and 3458-3457 primer pairs. The amplicons were digested with the restriction enzymes XbaI-XhoI and XhoI-EcoRI, respectively, and cloned into the mutagenic plasmid pGPI-SceI digested with XbaI and EcoRI giving rise to pDelL0352. Several deletion plasmids were created using a similar approach. To create pDelL0351, pDelL0350, pDelL0349, pDelL0339, pDelL0338, pDelL0337, and pDelL0336-33 (to delete BCAL0351, 0350, 0349, 0339, 0338, 0337 and BCAL0336-0333, respectively), PCR products were amplified using primers 3203-3177 and 3201-3202; 5190-5189 and 5188-5187; 5194-5193 and 5192-5191; 3948-3947 and 5178-5177; 5181-5182 and 5179-5180; 5185-5186 and 5184-5183; 5026-5025 and 5334-5333, respectively.

Deletion of BCAL0345 paralogs. To create pDelL1293 and pDelS0668 (to delete BCAL1293 and BCAS0668, respectively), PCR products were amplified using primers 4896-4895 and 4894-4893; 4902-4901 and 4900-4899, respectively.

Deletion of *vgrGs*. To create pDelL1165, pDelL1294, pDelL1355, pDelL1359, pDelL1362, pDelL2279, pDelM0043, pDelM0148, pDelM2254 and pDelS0667 (to delete BCAL1165, 1294, 1355, 1359, 1362, 2279, BCAM0043, 0148, 2254 and BCAS0667, respectively), PCR products were amplified using primers 3800-3801 and 4185-4186; 3059-3065 and 3066-3068; 3349-3354 and 5015-5016; 5017-5018 and 5019-5020; 5021-5022 and 5023-5024; 4305-4306 and 4308-4309; 4125-4126 and 4127-4128, 3759-3760 and 3761-3762; 4134-4135 and 4136-4137, 2863-3263 and 3267-2867, respectively.

Complementing plasmids. The complementing plasmids pL0345, pL1293, pM1857 and pS0668 were created as follows. BCAL0345, BCAL1293, BCAM1857 and BCAS0668 were PCR amplified using primer pairs 4905-4906, 4897-4898, 6207-6208 and 4903-4904, respectively. PCR products were digested with *Nde*I and *Xba*I and cloned into similarly digested pDA12.

SUPPLEMENTARY FIGURES

```

bcj_BCAL0345 1 ---MEELLFMYERELSELRRYSRDFAERYPKIAARLASEGHECEDPHVERMIESFALLG
bcj_BCAL1293 1 ---MDHLSSHYEREVGLLARSLADFAERREPDKIAARLGMSSGHVEDLHVDRMVQTFALLA
bcj_BCAS0668 1 MAIEPEELLPHSERELGLLRSTRFAELYPKIAARLAMSGEHSDDPHVERLIQSFALMC

bcj_BCAL0345 57 ARDNKLLDDDDYPEFTEALLEVLYPHYLRFPFPCSIAQFTF-ASFGQOETEPVVIERGTELK
bcj_BCAL1293 57 ARVDAKLLDDDYQCFTEALLELAYPHYLRTPVPSCAVASFDESVLFGQLTEPLITARGMMLD
bcj_BCAS0668 61 ARHDIRLEDEVPEFTHALINTHGAELRFPFSCMAQERVDRDSKQ-TEPRIVPRGTQLV

bcj_BCAL0345 116 SRPIREVOCRFRTAYDVTLPARISEARYTPVALAPSATVLFSNATCVISITFESLAQQL
bcj_BCAL1293 117 AN---AAPCRFRTYDVTLSPLRIYSARYSSATLAPAAARIPEVVTGIIISITFSESASQ
bcj_BCAS0668 120 AP---NSRLVVERTAADVTLVPLTVSGVRYATSTVAEMQITLPADTTGILSFTLTLTAFSA

bcj_BCAL0345 176 DLG-AIKLSTLRHLHGEQSFVAALTDCLFVNVLQAYVEPERNGRWTLRKLPIAQGFA
bcj_BCAL1293 174 AFDDALPSTFVRVHLSGERPVAALSDTLRLRASAAAYVEVDESGRWTRLSKVPLEAAGFA
bcj_BCAS0668 177 QFS--LAPDTVRHLAGEREVVAALADGVLMHATRAFEVLDCNGRWRRVD-MPLAAGFD

bcj_BCAL0345 235 ED DALDYE-AKSHPAVRLLEFYFAPPKDFVDFDLAATARAS--GRCORATLHLVQLD
bcj_BCAL1293 234 DGERLLEKQDDTSAQSFRLLEFYFAPPKDFVDFDLGRMRAARAERARRITLHVAQOG
bcj_BCAS0668 234 DADALLEPFRDNTAPFHLREYGAFFPFRDNLDDLARLKRLAG--GARRITLHLALAG

bcj_BCAL0345 292 VRSDSVARLLELELMASHFRLEFCTPVTNLFROHGEPPIRTHRAVSYPVIAEARL-AFAYE
bcj_BCAL1293 294 TAHDSGTAQLLATINTSTERLEFCTPVVNLFERAAIPIQLTSHDATYPIITPTPLATGIPLS
bcj_BCAS0668 292 VHPDSCAQRLLIAASADNLRLEFCTPVVNLFSSNAEPIETKAGQAYALKEFSLKTAATTE

bcj_BCAL0345 351 VYSIDSVKLVV-----QQAHESVIEFRPFYSLHHC-BAARICHYWFARRNDWVA
bcj_BCAL1293 354 VYSVEAVYLGERTKSGEDKAAIASHAAPRTQVWPVRAFSHARPMDSSAIYWLAVRDPETM
bcj_BCAS0668 352 IWSVDQVRRIT-----AQGAALPPPESLQHALCAAPGPYVIVLHDEARRA

bcj_BCAL0345 400 QKSE-----GYETEISIVDIDFEPSTPQTD-TLSLDLCTNRD
bcj_BCAL1293 414 PDGA-----LAESQLALVLDLKGQTAHPRHP-QVDVDVLAINGA
bcj_BCAS0668 398 PKPPESEPGKPGQALRGQATGARADGLRGLLALVNARGEFVDEAAQRQLDVLVLSCTNGN

bcj_BCAL0345 437 LPAMLAFLGEGGDIQEGGAQTSGLSLRRPTQSVRFERGRAHWRVLSHLALMHSLSVA
bcj_BCAL1293 451 MFSRLPIGAPDSDLLYEGSALACPTMLLSRPTLPALPRG-GALWRVLSALAPHPDLTR
bcj_BCAS0668 458 LADMRRER----QLAVRCDSCDELELLAQPSASPAPILRGELWELLSNLPQAARLNA

bcj_BCAL0345 497 HGLAPLKEMLTLDLRRITAVSMROTDGLVGVQRCGAVQWIPGKP-FATFVRGTEIRLITD
bcj_BCAL1293 510 TGLPALKEFLRFHAPRSSVVAQRCLDAASLCKPAIRWMSLDDHPSFVRGVEILLSVS
bcj_BCAS0668 513 EGLDELRKLCARFC-MFAPDAGRRFDALVSLSTERMRRWMPGKP-ASAFVQGLEVRIVLD

bcj_BCAL0345 556 EEFVVGASLASFVRVLSFFGLYVHLNSFVQLVVVSKRTGEEILRCRPRPTGESILA
bcj_BCAL1293 570 EAATRQVSLHRSVAVMDRFFGPIAQSNSIVQLVVLSAESDKELLRCAAPRPGTQPLV
bcj_BCAS0668 571 EQRFVQESLAGLGRVMDRLFSFYVPTSFVQIVLISAETGVVLRERGEFCAGSQPLI

```

Fig. S1 Aubert *et al.*

Sequence alignment of BCAL0345 and paralogs (BCAL1293 and BCAS0668). Sequence alignment was generated using ClustalW (Larkin *et al.*, 2007). Identical (black) and similar (grey) residues were illustrated using BOXSHADE (http://www.ch.embnet.org/software/BOX_form.html).

SUPPLEMENTARY REFERENCES

Aschtgen, M. S., Thomas, M. S. & Cascales, E. (2010). Anchoring the type VI secretion system to the peptidoglycan: TssL, TagL, TagP... what else? *Virulence* **1**, 535-540.

Aubert, D., MacDonald, D. K. & Valvano, M. A. (2010). BcsK_C is an essential protein for the type VI secretion system activity in *Burkholderia cenocepacia* that forms an outer membrane complex with BcsL_B. *J Biol Chem* **285**, 35988-35998.

Bonemann, G., Pietrosiuk, A., Diemand, A., Zentgraf, H. & Mogk, A. (2009). Remodelling of VipA/VipB tubules by ClpV-mediated threading is crucial for type VI protein secretion. *EMBO J* **28**, 315-325.

Boyer, F., Fichant, G., Berthod, J., Vandenbrouck, Y. & Attree, I. (2009). Dissecting the bacterial type VI secretion system by a genome wide in silico analysis: what can be learned from available microbial genomic resources? *BMC Genomics* **10**, 104.

Cascales, E. & Cambillau, C. (2012). Structural biology of type VI secretion systems. *Philos Trans R Soc Lond B Biol Sci* **367**, 1102-1111.

Craig, F. F., Coote, J. G., Parton, R., Freer, J. H. & Gilmour, N. J. (1989). A plasmid which can be transferred between *Escherichia coli* and *Pasteurella haemolytica* by electroporation and conjugation. *J Gen Microbiol* **135**, 2885-2890.

Durand, E., Zoued, A., Spinelli, S., Watson, P. J., Aschtgen, M. S., Journet, L., Cambillau, C. & Cascales, E. (2012). Structural characterization and oligomerization of the TssL protein, a component shared by bacterial type VI and type IVb secretion systems. *J Biol Chem* **287**, 14157-14168.

English, G., Byron, O., Cianfanelli, F. R., Prescott, A. R. & Coulthurst, S. J. (2014). Biochemical analysis of TssK, a core component of the bacterial Type VI secretion system, reveals distinct oligomeric states of TssK and identifies a TssK-TssFG subcomplex. *Biochem J* **461**, 291-304.

Felisberto-Rodrigues, C., Durand, E., Aschtgen, M. S., Blangy, S., Ortiz-Lombardia, M., Douzi, B., Cambillau, C. & Cascales, E. (2011). Towards a structural comprehension of bacterial type VI secretion systems: characterization of the TssJ-TssM complex of an *Escherichia coli* pathovar. *PLoS Pathog* **7**, e1002386.

Figurski, D. H. & Helinski, D. R. (1979). Replication of an origin-containing derivative of plasmid RK2 dependent on a plasmid function provided in *trans*. *Proc Natl Acad Sci USA* **76**, 1648-1652.

Flannagan, R. S., Linn, T. & Valvano, M. A. (2008). A system for the construction of targeted unmarked gene deletions in the genus *Burkholderia*. *Environ Microbiol* **10**, 1652-1660.

Larkin, M. A., Blackshields, G., Brown, N. P. & other authors (2007). Clustal W and Clustal X version 2.0. *Bioinformatics* **23**, 2947-2948.

Shalom, G., Shaw, J. G. & Thomas, M. S. (2007). *In vivo* expression technology identifies a type VI secretion system locus in *Burkholderia pseudomallei* that is induced upon invasion of macrophages. *Microbiology* **153**, 2689-2699.

Zoued, A., Durand, E., Bebeacua, C., Brunet, Y. R., Douzi, B., Cambillau, C., Cascales, E. & Journet, L. (2013). TssK is a trimeric cytoplasmic protein interacting with components of both phage-like and membrane anchoring complexes of the type VI secretion system. *J Biol Chem* **288**, 27031-27041.

Zoued, A., Brunet, Y. R., Durand, E., Aschtgen, M. S., Logger, L., Douzi, B., Journet, L., Cambillau, C. & Cascales, E. (2014). Architecture and assembly of the Type VI secretion system. *Biochim Biophys Acta*.

Additional Material for Reviewer

[Click here to download Additional Material for Reviewer: Aubert_T6SSactivity_merged-for editor.pdf](#)